



**HAL**  
open science

## **Silicon cycle in Indian estuaries and its control by biogeochemical and anthropogenic processes**

K.R. Mangalaa, Damien Cardinal, Julien Brajard, D.B. Rao, N.S. Sarma, Irina DjouraeV, G. Chiranjeevulu, K. Narasimha Murty, V. V. S. S. Sarma

► **To cite this version:**

K.R. Mangalaa, Damien Cardinal, Julien Brajard, D.B. Rao, N.S. Sarma, et al.. Silicon cycle in Indian estuaries and its control by biogeochemical and anthropogenic processes. *Continental Shelf Research*, 2017, 148, pp.64-88. 10.1016/j.csr.2017.08.011 . hal-01651900

**HAL Id: hal-01651900**

**<https://hal.sorbonne-universite.fr/hal-01651900>**

Submitted on 29 Nov 2017

**HAL** is a multi-disciplinary open access archive for the deposit and dissemination of scientific research documents, whether they are published or not. The documents may come from teaching and research institutions in France or abroad, or from public or private research centers.

L'archive ouverte pluridisciplinaire **HAL**, est destinée au dépôt et à la diffusion de documents scientifiques de niveau recherche, publiés ou non, émanant des établissements d'enseignement et de recherche français ou étrangers, des laboratoires publics ou privés.

# Silicon cycle in Indian estuaries and its control by biogeochemical and anthropogenic processes

K. R. Mangalaa<sup>1</sup>, D. Cardinal<sup>1\*</sup>, J. Brajard<sup>1</sup>, D.B. Rao<sup>2</sup>, N.S. Sarma<sup>2</sup>, I. Djouaev<sup>1</sup>, G. Chiranjeevulu<sup>2</sup>, K. Narasimha Murty<sup>2</sup>, and V.V.S.S. Sarma<sup>3</sup>

<sup>1</sup> Sorbonne Universités (UPMC, Univ. Paris 06)-CNRS-IRD-MNHN, LOCEAN Laboratory, CP100, 4 place Jussieu, F-75252 Paris cedex 5, France

<sup>2</sup> Marine Chemistry Laboratory, Andhra University, Visakhapatnam - 530 003, India

<sup>3</sup> National Institute of Oceanography, Regional Centre, 176 Lawsons Bay Colony, 530 017 Visakhapatnam, India

\* Corresponding author

## Abstract

We study the silicon biogeochemical cycle and its associated parameters in 24 and 18 Indian estuaries during dry and wet periods respectively. We focus more specifically on dissolved Si (DSi), amorphous Si (ASi), lithogenic Si (LSi), Particulate Organic Carbon (POC), Total Suspended Material (TSM), Dissolved Inorganic Nitrogen (DIN), salinity and fucoxanthin, a marker pigment for diatoms. Overall, we show that the estuaries have strong inter and intra variability of their biogeochemical parameters both seasonally and along salinity gradients. Based on Principal Component Analysis and clustering of categorised (upper and lower) estuaries, we discuss the four major processes controlling the Si variability of Indian estuaries: 1) lithogenic supply, 2) diatom uptake, 3) mixing of sea water and, 4) land use. The influence of lithogenic control is significantly higher during the wet period than during the dry period, due to a higher particle supply through monsoonal discharge. A significant diatom uptake is only identified in the estuaries during dry period. By taking into account the non-conservative nature of Si and by extrapolating our results, we estimate the fluxes from the Indian subcontinent of DSi, ASi, LSi to the Bay of Bengal ( $211 \pm 32$ ,  $10 \pm 4.7$ ,  $2028 \pm 317$  Gmol) and Arabian Sea ( $80 \pm 15$ ,  $7 \pm 1.1$ ,  $1717 \pm 932$  Gmol). We show the impact of land use in watersheds with higher levels of agricultural activity amplifies the supply of Si to the coastal Bay of Bengal during the wet season. In contrast, forest cover and steep slopes cause less Si supply to the Arabian Sea by restricting erosion when entering the estuary. Finally, Si:N ratios show that nitrogen is always in deficit relative to silicon for diatom growth, these high Si:N ratios likely contribute to the prevention of eutrophication in the Indian estuaries and coastal sea.

## Highlights

- Strong seasonal inter and intra estuarine variability of biogeochemical parameters
- Non-conservative behaviour of particulate Si fluxes during wet and dry seasons
- Significant control by diatoms during dry season on Si cycle
- Important influence of land use during wet season on dissolved and particulate Si

41 • High Si:N ratios may prevent eutrophication in Indian estuaries and coasts

42

43 **Keywords**

44

45 Amorphous silica

46 Weathering

47 Diatoms

48 Land use

49 Monsoon

50 Land-to-ocean continuum

51

52

## 53 1. Introduction

54

55 Silicon (Si) constitutes 28% of the Earth's crust and it is the second most abundant element (Wedepohl et al.,  
56 1995). In aquatic ecosystems, Si is released through chemical weathering in dissolved form and by erosion as  
57 particles with high Si content either as primary residual minerals (e.g. quartz, feldspars) or as secondary  
58 minerals (e.g. clays). This particulate Si mineral pool is referred to as lithogenic silicon (LSi) and it is often  
59 neglected in biogeochemical budgets because of its low reactivity. Silicic acid (or dissolved silicon, DSi), is a  
60 key nutrient for diatoms, sponges, radiolarians and other aquatic organisms with a siliceous skeleton.  
61 Additionally, terrestrial plants take up DSi and precipitate silica particles (called phytoliths) inside cells.  
62 Diatoms and phytoliths are considered to be the major source of Biogenic Silica (BSi) supply to the coastal  
63 water (Ragueneau et al., 2000). In the ocean, diatoms play a dominant role amongst phytoplankton in carbon  
64 uptake (75% of coastal primary production; Nelson et al., 1995) and sediment burial because of their larger size  
65 and refractory structure (Ducklow et al., 2001). Carbon and silicon cycles are thus inter-related since diatoms  
66 presently play a dominant role in carbon sequestration whereas weathering connects C and Si cycles at long-  
67 term geological cycles (Berner, 1992).

68

69 Today,  $6.2 \pm 1.8 \text{ Tmol.yr}^{-1}$  of DSi and  $1.1 \pm 0.2 \text{ Tmol.yr}^{-1}$  of BSi are transported by rivers to the estuaries  
70 (Tréguer and De La Rocha, 2013). The amorphous silica (ASi) is mostly of biogenic origin (phytoliths, diatoms,  
71 sponge spicules) and relatively dissolvable in the aquatic ecosystems. ASi or BSi transport through rivers has  
72 often been neglected compared to DSi, but some studies clearly show a substantial contribution of ASi flux to  
73 the ocean (e.g. Conley, 1997). For instance, in some rivers, ASi flux can exceed 50% of DSi flux (Frings et al.,  
74 2014) and may thereby significantly contribute to the global Si cycle. Phytoliths can also contribute significantly  
75 to the BSi pool in rivers (Cary et al., 2005; Ran et al., 2015). According to the revised oceanic silicon cycle  
76 (Tréguer & De La Rocha, 2013), and neglecting LSi, 80% of external Si supply to the ocean is coming from  
77 rivers either as ASi or DSi. About 21% ( $1.5 \pm 0.5 \text{ Tmol Si year}^{-1}$ ) is trapped in the estuaries, yielding a net  
78 supply of  $5.8 \pm 1.9 \text{ Tmol Si year}^{-1}$  to the ocean (Tréguer & De La Rocha, 2013). One can notice that there exist  
79 large uncertainties regarding the above fluxes (ca.  $\pm 33\%$ ) due to the poor understanding of the seasonal cycle of  
80 Si in many rivers and the absence of data, particularly for ASi, as well as the non-conservative behaviour of  
81 DSi in the estuaries before entering the coastal region (Conley, 1993; Chou and Wollast, 2006; Dürr et al.,  
82 2011).

83

84 By definition, an estuary is a semi-enclosed coastal body having a open connection with both sea water and  
85 fresh water from land drainage up to the tidal freshwater reach. The estuarine ecosystems are highly productive,  
86 with a rich biodiversity. They are characterized by profound changes in the hydro-chemical properties and  
87 biological processes. Anderson (1986) stated that biological productivity is higher in the tidal freshwater reach  
88 because of reduced turbidity (and hence reduction of its limiting effect on light) as opposed to the turbidity  
89 maximum region along the increasing salinity gradient. Diatom growth may affect DSi concentration in the  
90 estuaries through uptake (Admiraal et al., 1990; Conley, 1997; Hughes et al., 2011). In addition, anthropogenic  
91 activities such as damming may decrease DSi by favouring BSi retention in the reservoirs (Conley 2002; Friedl  
92 et al., 2004; Humborg et al., 2006; Laruelle et al., 2009; Hughes et al 2012). In contrast, deforestation (Conley et

93 al., 2008) and amplified erosion (Xiangbin et al., 2015) may increase the supply of both DSi and BSi to the  
94 coastal system. Moreover, heightened fertilizer usage (Li et al., 2007) results in a supply of excess N and P over  
95 Si leading to the development of non-diatom blooms favouring HAB (Harmful Algal Blooms) and  
96 eutrophication, major threats to the base of food chain (Garnier et al., 2010; Howarth et al., 2011).

97

98 The eutrophication potential has been increasing for Indian estuaries over the last four decades, compared to the  
99 temperate estuaries (Europe and USA), because of increase in agriculture, fast urbanization and insufficient  
100 sewage treatment. The ICEP (Indicator of Coastal Eutrophication Potential) is based on the N:Si or P:Si ratios of  
101 riverine inputs to the coast (Garnier et al., 2010). A higher ICEP would favour eutrophication since Si would be  
102 limiting. Hence, ignoring the ASi fraction that could dissolve and partly counterbalance the excess of N and P  
103 relative to Si, may lead to an overestimated eutrophication potential. Compared to N, P and C, the Si cycle is  
104 less well understood and needs to be approached by considering the above processes along the land-ocean  
105 continuum for better determination of the health and functioning of the ecosystems. There is a lack of data,  
106 especially in the tropical regions, which contribute to 74% of riverine Si input (Tréguer et al., 1995).

107

108 Indian tropical estuaries differ significantly from other estuaries in terms of rainfall, discharge and land use. The  
109 Indian subcontinent is rich with high mountain ranges, widespread plateaus and extensive plains traversed by  
110 large rivers. India has ~220 major and minor estuaries with varying size and shape along the ~7500 km coastline  
111 (Sarma et al., 2012; Rao et al., 2013). India experiences seasonally reversing monsoonal systems called  
112 southwest or summer monsoon (June to September) and northeast or winter monsoon (November to February).  
113 In the Indian subcontinent, 75% of annual rainfall is received during southwest monsoon and the remaining 25%  
114 during northeast monsoon (Attri et al., 2010). Except for the glacial rivers such as Ganges and Brahmaputra,  
115 Indian rivers are strongly influenced by the precipitations during southwest and northeast monsoons and most  
116 estuaries receive a huge freshwater flux in a limited period of time. These estuaries are therefore referred to as  
117 monsoonal estuaries. For instance, southwestern India receives more rainfall (~3000 mm/yr) than northeastern  
118 (1000-2500 mm/yr), southeastern (300-500 mm/yr) and northwestern India (200-500 mm/yr) (Soman and  
119 Kumar, 1990). The variability of the estuarine discharge induced by rainfall is discussed in Sarma et al. (2014).  
120 During the peak monsoon period the entire estuary may be filled with freshwater with no vertical salinity  
121 gradient and exhibit riverine and non-steady state behaviour (Vijith et al., 2009; Sridevi et al., 2015). On the  
122 other hand, the upper estuary gets dried up due to weak discharge, allowing the penetration of seawater during  
123 the dry period. The Indian subcontinent is bounded by the Arabian Sea on the west and the Bay of Bengal on the  
124 east and receives  $0.3 \times 10^{12} \text{ m}^3$  freshwater influx from rivers to the former basin and  $1.6 \times 10^{12} \text{ m}^3$  to the latter  
125 basin (Krishna et al., 2016). In addition to freshwater influx, the glacial and monsoonal rivers supply a  
126 enormous load of suspended matter of around  $1.4 \times 10^9$  tons to the Bay of Bengal and  $0.2 \times 10^9$  tons into the  
127 Arabian Sea respectively (Nair et al., 1989; Ittekkot et al., 1991).

128

129 Agriculture is the main economic activity in India and the most common land use (61% of total watershed —  
130 Central Water Commission report, 2014), with a massive consumption of fertilizers (it ranks second in the world  
131 — Ministry of Agriculture report, 2012-13), which end up in the estuaries and coastal water (Sarma et al.,  
132 2014). This may provoke an imbalanced nutrient supply to the coastal waters. Apart from the fertilizer use,

133 agriculture also favours erosion. Around  $5.3 \times 10^9$  tonnes of soil is eroded annually, of which 29% enters the  
134 sea, 10% is retained by reservoirs and the remaining 61% are displaced without reaching the ocean yet (Ministry  
135 of Agriculture report, 2012-13). The rivers in India are heavily dammed to meet irrigation, domestic and  
136 hydroelectric demands. India ranks fourth in total number of dams in the world (CWC, 2009) and damming may  
137 cause nutrient retention via biological uptake and sedimentation, thereby also altering the nutrient supply and in  
138 fine the phytoplankton diversity and production in the estuaries as well as adjacent coastal ocean. However,  
139 despite high consumption of fertilizers in the Indian subcontinent, the concentrations and fluxes of DIN and DIP  
140 to the coastal waters is much lower than e.g. in the China Sea. This could be caused by a high nutrient supply  
141 during the short 2-3 peak monsoon months avoiding eutrophication because of the high turbidity and quick  
142 dilution into the ocean (Rao and Sarma, 2013; Krishna et al., 2016) and/or a high Si:N ratios preventing non-  
143 diatom blooms (Garnier et al., 2010).

144

145 So far, there are no studies on the ASi and LSi distribution in the Indian estuaries other than Ganges (Frings et  
146 al., 2014). Here, we will mainly focus on 1) Seasonal variability of ASi, DSi and LSi in ca. 20 estuaries draining  
147 into the Bay of Bengal and Arabian Sea. 2) Understanding the associated biogeochemical processes and the  
148 impact of land use on Si variability. And, lastly, 3) Estimating the flux of ASi, DSi and LSi from the Indian sub-  
149 continent to the North Indian coastal ocean and their contribution to the global Si budget.

150

## 151 **2. Materials and Methods**

152

153 In this study, the estuaries are first categorized into four groups based on their geographic location: northeast  
154 (NE), southeast (SE), southwest (SW), northwest (NW) (Table 1 and details therein). These estuaries were  
155 studied before, for dissolved inorganic nitrogen (DIN) fluxes, greenhouse gas fluxes and source of organic  
156 matter (Sarma et al., 2012, 2014; Rao and Sarma, 2013; Krishna et al. 2016).

157

158

Name of River/Estuary	Catchment area km <sup>2</sup>	Length km	% Agriculture 2005-2006	% Forest	Slope %	Discharge		Runoff		
						Dry period km <sup>3</sup>	Wet period km <sup>3</sup>	Dry period (m)	Wet period (m)	
<b>Rivers flowing in Bay of Bengal, East coast estuaries</b>										
Northeast	Haldia (Hal)	10200	NA	65 (Ganges)	16 (Ganges)	NA	12.6	1.24	37	3.71
	Subernereka (Sub)	29196	448	54	29	0.13	3.1	0.11	9.3	0.32
	Baitharani (Bai)	10982	355	52	34	0.25	NA	NA	NA	NA
	Mahanadi (Maha)	141600	851	54	33	0.10	16 ± 0.7	0.12	50 ± 9	0.35
	Rushikulya (Rush)	7700	165	60	26	0.61	0.6 ± 0.4	0.08	1.1 ± 0.3	0.15
	Vamsadhara (Vam)	10830	254	"	"	NA	1.1 ± 0.1	0.10	2.4 ± 0.8	0.22
Nagavalli (Nag)	9510	256	"	"	0.51	0.7 ± 0.3	0.08	1.2 ± 0.6	0.13	
Southeast	Krishna (Kris)	258948	1400	76	10	0.10	3.6 ± 0.1	0.01	66 ± 10	0.26
	Godavari (God)	312812	1465	60	30	0.07	21 ± 1.4	0.07	90 ± 26	0.29
	Penna (pen)	55213	597	59	20	0.13	0.6 ± 0.005	0.01	5.7 ± 0.7	0.10
	Ponnaiyar (pon)	16019	292	67	15	0.31	0.1 ± 0.005	0.01	1.5 ± 0.6	0.09
	Vellar (Vel)	8922	210	"	"	0.43	0.3	0.04	0.6 ± 0.1	0.06
	Cauvery (Cau)	81155	800	66	21	0.17	4.3 ± 0.2	0.05	17 ± 2.1	0.21
	Ambullar (Amb)	NA	NA	67	15	NA	NA	NA	NA	NA
Vaigai (Vai)	7741	258	"	"	0.47	NA	NA	NA	NA	
<b>Rivers flowing in Arabian sea, west coast estuaries</b>										
Southwest	Kochi Backwater (KBW)	5243	228	51	35	NA	5.1 ± 0.2	0.96	7.2 ± 0.4	1.38
	Chalakudi (cha)	1704	130	"	"	0.96	0.5 ± 0.1	0.30	1.4 ± 0.4	0.83
	Bharathapula (Bha)	5397	251	"	"	0.98	1.7 ± 0.03	0.32	3.3 ± 0.2	0.62
	Netravathi (Net)	3657	103	"	"	0.97	1.5 ± 0.1	0.42	9.5 ± 1.5	2.59
	Kali (Kali)	4943	184	44	35	NA	0.7	0.14	4.1 ± 0.7	0.83
	Zuari (Zua)	1152	34	"	"	NA	0.6	0.48	2.7 ± 0.7	2.34
	Mandovi (Man)	1895	50	"	"	1.20	0.6 ± 0.1	0.30	2.7 ± 0.7	1.45
Northwest	Tapti (Tap)	65145	724	66	24	0.10	5.2 ± 0.1	0.08	9.7 ± 0.5	0.15
	Narmada (Nar)	98796	1312	57	33	0.08	8.9 ± 0.5	0.09	37 ± 10	0.37
	Mahisagar (Mahi)	34842	583	64	19	0.09	1.2 ± 0.03	0.04	9.8 ± 5.4	0.28
	Sabarmathi (Sab)	21674	371	75	12	0.21	0.9 ± 0.1	0.04	2.8 ± 1.3	0.13

159

160 **Table 1.** List of estuaries sampled and the general characteristics of their watershed. The dry and wet  
161 discharges are re-calculated from the annual total discharge reported by Krishna et al. (2016) using the  
162 percentage contribution during wet period that is calculated from the Indian water portal (<http://www.india-wris.nrsc.gov.in/>) (see text for more details). The runoff is calculated by dividing the discharge (m<sup>3</sup>) by the  
163 surface area of the watershed (m<sup>2</sup>). The slope of the watershed is calculated by dividing the elevation of  
164 watershed by the length of the river. Except annual total discharge, all data is obtained from <http://www.india-wris.nrsc.gov.in/>. For some of the watersheds, the land-use data were grouped for adjacent rivers.

167

## 168 2.1 Sampling and ancillary biogeochemical parameters

169

170 24 estuaries were sampled along the entire coastline of India during the dry (NE monsoon, Jan-Feb 2012) and 18  
171 during the wet period (SW monsoon, July-August 2014) (Fig. 1). In each estuary, generally three to five samples  
172 were collected across the salinity gradient from near-zero salinity to the mouth of the estuary. The mode of  
173 sampling was adapted to circumstances such as boat/ferry availability and accessibility (e.g. restricted due to  
174 heavy discharge). Some were sampled directly from shore, but most samples were obtained from the middle of  
175 the stream (a strategy we have favoured whenever possible). Temperature and salinity were measured by using  
176 portable CTD for some estuaries (Sea Bird Electronics, SBE 19 plus, USA) and portable pH and conductivity  
177 electrode (WTW, MultiLine P4) were used in other estuaries. The latter was calibrated with CTD to calculate  
178 the salinity. Surface water samples were collected for Dissolved Inorganic Nitrogen (DIN), Dissolved Inorganic  
179 Phosphorus (DIP), silicic acid (DSi), Total Suspended Material (TSM) and phytoplankton pigments using  
180 Niskin (5L) sampler. The DIP and DIN samples were preserved with saturated mercuric chloride after filtration  
181 to stop bacterial activity, and transported to the laboratory for analysis. DIP and DIN were analysed using  
182 spectrophotometer following Grasshoff et al. (1999). Depending on the turbidity, 100 to 500 ml of water was

183 filtered with a cellulose nitrate filter for dry period samples (pore size 0.45  $\mu\text{m}$ ) and polyethersulfone Supor (0.2  
 184  $\mu\text{m}$ , Pall Corporation) filter for wet period. TSM is calculated by subtracting the weight (recorded before  
 185 sampling) of each filter. Subsequently, amorphous silica (ASi) is measured from an aliquot of the filter. Another  
 186 500 ml of each sample was filtered through Glass Fibre membrane (GF/F; 0.7  $\mu\text{m}$  pore size; Whatman) under  
 187 gentle vacuum, for the measurement of photosynthetic pigments. Phytoplankton pigments are tracers of the type  
 188 of phytoplankton. Fucoxanthin is a pigment present in the bacillariophyceae group and as such considered  
 189 indicative for the presence of diatoms (Ansotegui et al., 2001; Wysocki et al., 2006; Zhang et al., 2015).  
 190 Fucoxanthin is measured using High Performance Liquid Chromatography (HPLC-series 1200 Agilent  
 191 Technologies) following Heukelem and Thomas (2001).



192  
 193 **Fig. 1:** Map showing the monsoonal estuaries with main watershed limits (dark blue lines) and rivers (light blue  
 194 lines). Samples collected during dry (circles) 2012 and wet (stars) 2014 periods. Estuaries shown as triangles,  
 195 while sampled during the 2014 wet period, are considered dry because of low discharge (see text).

196  
 197 **2.2 Water Discharge**

198  
 199 The water discharge in Indian estuaries is highly dependant on the monsoonal rainfall and varies between 0.1 to  
 200 20 km<sup>3</sup> and 0.6 to 90 km<sup>3</sup> during dry (non-monsoon) and wet (monsoon) periods respectively (Table 1). The dry  
 201 and wet discharges are re-calculated from the annual total discharge reported by Krishna et al. (2016) because



202 their data is closest to our sampling sites. To separate the wet and dry period discharge for each estuary, we  
203 calculate their relative contributions using data from the Indian water portal ([http://www.india-  
205 wris.nrsc.gov.in/](http://www.india-<br/>204 wris.nrsc.gov.in/)). As this portal contains no discharge data for the wet sampling period (July-August 2014), 10  
206 years average data for the four monsoon months (June-September for SW monsoonal rivers, September-  
207 December for NE monsoonal rivers) as well as 10 years average for the eight remaining low discharge months  
208 are used instead. .

209 Large differences in the amount of precipitation, water use, length and origin of the river are responsible for a  
210 high regional variability of discharge in the Indian estuaries.(Sarma et al., 2014). At the time of sampling,  
211 discharge was typically high during wet period in all estuaries except the southeastern estuaries (Ponnaiyar,  
212 Vellar, Vaigai and Cauvery) that have low discharge all year long because of limited rainfall during the  
213 southwest monsoon and high water use upstream. Moreover, SW monsoon was particularly late in 2014 and at  
214 the time of sampling, Krishna (SE) estuary was still at low discharge. The “wet” period sampling of these five  
215 estuaries will therefore be treated as dry period, since discharge was indeed low. During actual dry period  
216 sampling, discharge was very low in all the estuaries (Table 1).

217

### 218 **2.3 Measurement of Amorphous (ASi) and Lithogenic silica (LSi)**

219

220 There is a growing interest in understanding the Si biogeochemical cycle and analysis of ASi has become  
221 essential in aquatic and soil biogeosciences. The correct measurement of ASi in the suspended matter is required  
222 in order to recognize the fate and forms of Si along the land-to-ocean continuum. The diversity of silicate  
223 minerals can bias ASi estimates, making its measurement challenging, especially in estuaries and rivers. Among  
224 the several existing protocols, the most widely used methods for ASi determination in suspended matter are wet  
225 chemical alkaline digestions using  $\text{Na}_2\text{CO}_3$  (Conley, 1998) or  $\text{NaOH}$  (Ragueneau et al., 2005). However, the  
226 resulting ASi concentrations can sometimes differ by an order of magnitude, depending on the protocol. Indeed,  
227 these chemical leaching protocols do not allow to differentiate biogenic silica (BSi) from ASi; hence when we  
228 use the term ASi to represent the Si extracted by digestion process, it includes BSi. We use the method  
229 described by Ragueneau et al. (2005) because it was developed especially for suspended matter with high  
230 silicate mineral contents.

231

232 For ASi measurement, chemical leaching is performed on a known fraction of the filter used to measure TSM.  
233 The filter aliquots were subjected to a wet alkaline digestion process, in which the released aluminium allows to  
234 correct the lithogenic contribution (Ragueneau et al., 2005). This method relies on three assumptions, 1) All  
235 aluminium measured is derived from silicate minerals, 2) All the biogenic silica is dissolved during first  
236 digestion, so the second leach should be representative of the Si:Al ratio of silicate minerals only and 3) Silicate  
237 minerals removed during second digestion have the same Si:Al ratio as those dissolved during the first  
238 digestion. Uncertainty on ASi measurement is estimated to be ~10%. All silicon concentrations were measured  
239 by spectrophotometer. We obtain a mean measured Si concentration of  $112.8 \pm 2.68 \mu\text{M}$ ,  $n=82$  (97.4%  
240 reproducibility) for the certified reference material (PERADE-09, supplied by environment Canada, lot no:  
241 0314, with  $\text{Si} = 109.96 \pm 6.97 \mu\text{M}$ ). .

242

243 The ASi measured is below detection limit or yielding negative values in the case of 41 (out of 143) samples of  
244 the dry period and 14 (out of 48) samples of the wet period. This is caused by the high lithogenic contribution  
245 during the first step, leading to an overestimation of the correction. It does not necessarily mean that the ASi  
246 concentration is low, since the detection limit depends more on the LSi contamination during the first leaching  
247 (with this contamination being correlated to the total LSi concentration) than the ASi content itself.

248

## 249 **2.4 Statistical Analysis**

250

251 Significant seasonal differences for all the studied parameters are identified using Excel-T-test assuming  
252 unequal variance and are reported with a significance level of p-value < 0.05. Standard deviations around mean  
253 value are given as  $\pm 1 \sigma_D$  in all tables. Similarly, the significance level for correlations is calculated using  
254 degrees of freedom (number of data) at 95% confidence level. Coefficients of determination ( $R^2$ ) of linear  
255 regressions are given only for such significant relationships.

256

257 We use the ordination analysis (Principal Component Analysis – PCA, and clustering on PCA results) for the  
258 discussion of biogeochemical processes. However, negative and missing data are not allowed in this processing.  
259 Therefore, the ASi negative values were calculated using the best linear relationship between ASi and  
260 fucoxanthin for the dry period and between ASi and TSM for the wet period (see § Results). These values,  
261 recalculated for negative ASi values, are only used for PCA and clustering interpretations (§ 3.2, 4.3 and 4.4)  
262 but not for the comparison of concentrations with literature, Si:N ratios and flux calculations (§4.1, 4.2 and 4.5).

263

264 For statistical interpretation (PCA and clustering), we separate all the estuaries into two main categories. We  
265 consider separately upper (salinity<5) and lower (salinity>5) estuaries categories for the following reasons: (i)  
266 the low salinity can be representative of the freshwater end-member, i.e. what is supplied to the estuary from  
267 rivers with little influence of seawater on concentrations (seawater contribution being max. 11%) or processes  
268 like flocculation, turbidity, marine phytoplankton seeding, etc. (ii) the second category (salinity >5) should  
269 indeed be the most representative of processes specific to estuarine systems since it has a large salinity gradient.  
270 This category should more particularly highlight the processes controlled by seawater intrusion which can have  
271 a significant influence, e.g. on estuarine turbidity maximum for salinity only slightly above 5 (Schoelhamer,  
272 2001; Sarma et al., 2012; Suja et al., 2015; Shynu et al., 2015). Moreover, the higher salinity of the samples  
273 from this category can also allow better estimation of the actual supply to the coastal ocean.

274

275 In addition, the estuaries holding more than one sample point under the same salinity category were averaged, to  
276 avoid repetition of the estuary in different clusters of the same category. Finally, before applying the ordination  
277 method, all the data is normalised and standardised (scaling and centering) in order to avoid the differences in  
278 data dimensions. Salinity, DSi, ASi, LSi, fucoxanthin, TSM, DIN and POC are used to identify the main  
279 biogeochemical processes (e.g., biological or non-biological) that govern the ASi, LSi and DSi contents. In a  
280 second statistical processing, land use and other main watershed characteristics features are compared to the  
281 same ASi, LSi and DSi contents to assess their impact on the Si cycle.

282

283 Hierarchical clustering on PCA results is performed in order to group the estuaries based on their similar  
284 behaviour and to deliver evidence regarding the dominant variable(s) in each cluster. The PCA and clustering on  
285 PCA results are performed using the R statistical program (<https://www.r-project.org/>) version 0.98.1103 (using  
286 FactoMineR package). In our study, PCA combined with cluster analysis, provided a synthetic classification of  
287 estuaries in response to the respective characterizing variables. Generally, we consider only such PC axes for  
288 which the Eigen values are greater than 1 while explaining the variability of biogeochemical parameters.

289

290 For each cluster, the ratio between the mean of the cluster and the overall mean of the category estuary  
291 (hereafter  $\text{ratio}_{(\text{mean})}$ ) is calculated. This ratio gives the most influent or characteristic variable(s) of the cluster.  
292 The ratio departing from 1 indicates either a strong enrichment ( $\text{ratio} \gg 1$ ) or a strong depletion ( $\text{ratio} \ll 1$ ) of  
293 that particular variable characterising the cluster. Note that all dominant variables are determined at the  
294 significance level of  $p < 0.05$ . Hence, thereafter, whenever the p-value is not given, is indicative of  $p < 0.05$ .

295

### 296 **3. Results**

297

298 Tables 2 and 3 provide the results of DSi, ASi, LSi, TSM, fucoxanthin, DIN and POC concentrations averaged  
299 ( $\pm \sigma_D$ ) for each estuary during the dry and wet periods respectively, while individual data is provided as a graph  
300 in Appendix A.

301

#### 302 **3.1 Seasonal variability**

303

##### 304 **3.1.1. Dissolved Silicon (DSi)**

305

306 The average DSi concentration of Indian upper estuaries (salinity  $< 5$ , considered representative of the  
307 freshwater river end-member) is  $213 \pm 139 \mu\text{M}$  during the dry period and  $163 \pm 88 \mu\text{M}$  during the wet period.  
308 During the dry period, the concentration of DSi is associated with greater variability compared to the wet period.  
309 During the dry period, there is a significantly higher DSi concentration in the eastern estuaries ( $179 \pm 142 \mu\text{M}$ )  
310 compared to the western ( $88 \pm 63 \mu\text{M}$ ) estuaries ( $p < 0.001$ ). In contrast, there is no such significant difference  
311 between east ( $143 \pm 43 \mu\text{M}$ ) and west ( $151 \pm 90 \mu\text{M}$ ) during the wet period ( $p = 0.7$ ).

312

	Name of river/Estuary	Salinity		DSi		ASi		LSi		TSM		Fucoxanthin		DIN		POC	
		Avg	SD (±)	µM	SD (±)	µM	SD (±)	µM	SD (±)	mg/l	SD (±)	µg/l	SD (±)	µM	SD (±)	µM	SD (±)
		Dry period															
Rivers Flowing in to Bay of Bengal, East coast	North east																
	Haldia	4.7	0.9	88	42	NA		875	729	143	117	0.3	0.1	29	4	231	92
	Subernereka	4.3	0.5	159	12	7.0	7.6	189	109	30	7	1.5	0.5	9	2	104	20
	Baitharani	17.5	4.4	37	12	0.6	0.7	207	85	56	13	0.7	0.5	10	3	135	27
	Rushikulya	20.4	2.8	63	28	1.4	0.4	54	12	27	2	0.4	0.1	7	2	57	17
	Vamsadhara	11.6	11.7	189	165	2.2	1.6	48	24	22	8	0.5	0.2	4	1	59	8
	Nagavalli	6.4	10.2	306	163	3.7	0.6	30	11	8	4	2.1	0.5	12	3	64	29
	Mahanadi	7.3	4.0	100	48	0.8	0.3	53	30	16	7	0.3	0.2	6	2	60	20
	South east																
	Krishna	15.8	8.3	113	97	5.0	4.7	50	42	52	34	1.2	1.4	20	21	54	9
	Cauvery	7.9	7.6	285	89	8.8	3.6	60	42	23	9	5.2	4.1	6	5	127	22
	Penna	9.8	9.8	140	73	3.5	4.0	36	32	14	11	1.9	1.3	13	6	63	0
	Ponnaiyar	5.2	9.2	389	187	17.4	18.9	105	121	77	25	8.6	7.1	9	4	106	12
	Vellar	10.1	10.6	298	179	6.9	3.1	105	57	53	37	2.9	2.4	13	11	203	61
Vaigai	11.6	8.6	154	59	NA		133	59	67	13	0.3	0.3	10	3	124	0	
Ambullar	4.2	0.0	317	5	2.5	0.7	40	5	17	14	0.2	0.1	7	1	95	23	
South west																	
Kochi BW	8.4	9.4	79	33	2.1	1.8	43	28	76	29	1.8	2.0	13	7	50	12	
Bharathapuzha	10.8	12.6	74	32	4.9	3.1	78	37	32	18	1.1	1.2	5	6	98	40	
Chalakudy	14.7	11.9	57	13	1.1	0.7	15	7	17	16	0.5	0.4	7	3	50	6	
Netravathi	8.0	12.0	90	32	3.4	1.4	115	118	29	25	2.7	1.9	5	2	74	26	
Kali	1.6	1.5	89	32	1.1	0.8	26	12	63	4	0.4	0.5	20	15	55	3	
Zuari	20.7	13.2	42	17	1.9	3.2	30	13	51	17	1.6	1.2	10	2	66	6	
Mandovi	20.9	8.5	38	20	1.8	2.1	29	15	42	19	2.4	3.2	12	5	45	8	
North west																	
Tapti	9.0	15.3	136	76	NA		1393	1306	418	448	1.2	1.4	29	14	NA		
Narmada	3.8	7.3	164	50	NA		171	124	22	16	0.7	0.5	37	6	NA		
Mahisagar	0.2	0.0	278	4	0.7	0.3	42	21	28	22	0.8	0.9	82	1	NA		
Sabarmathi	13.5	19.0	127	54	NA		1482	214	209	177	5.2	0.0	49	14	NA		
Dry upper overall mean																	
Dry estuary overall mean																	

313

314 **Table 2:** Variability of Salinity, Dissolved Silicon (DSi), Amorphous silica (ASi), Lithogenic silica (LSi), Total  
315 Suspended Matter (TSM), fucoxanthin, Dissolved inorganic Nitrogen (DIN) and Particulate Organic Carbon  
316 (POC) in the estuaries during the dry period. NA indicates non-availability of data.

317

	Name of Estuary	Salinity		DSi		ASi		LSi		TSM		Fucoxanthin		DIN		POC	
		Avg	SD (±)	µM	SD (±)	µM	SD (±)	µM	SD (±)	mg/l	SD (±)	µg/l	SD (±)	µM	SD (±)	µM	SD (±)
		Wet period															
Rivers Flowing in Arabian sea, west coast	North east																
	Haldia (ganges)	3.6	2.0	113	9	9.8	7.1	2076	367	566	272	0.5	0.1	29.0	18.9	131	35
	Subernereka	6.2	5.5	150	43	12.6	11.5	443	196	67	29	0.7	0.4	18.5	12.3	41	14
	Rushikulya	10.6	9.2	170	77	19.1	29.6	604	932	90	125	0.4	0.5	19.3	11.5	35	37
	Mahanadi	2.6	4.3	134	30	NA		1227	471	185	59	--	--	28.7	31.2	68	8
	South east																
	Godavari	0.6	0.6	147	13	22.3	16.8	1338	193	200	32			54.1	16.9	76	9
	krishna	Considered as Dry period because of No runoff and no rainfall during sampling															
	Cauvery	Considered as Dry period because of No runoff and no rainfall during sampling															
	Penna	Considered as Dry period because of No runoff and no rainfall during sampling															
	Ponnaiyar	Considered as Dry period because of No runoff and no rainfall during sampling															
	Vellar	Considered as Dry period because of No runoff and no rainfall during sampling															
	South west																
	Kochi BW	4.6	7.0	101	16	NA		294	204	50	30	0.7	0.6	38.0	25.7	100	27
Netravathi	0.1	0.0	130	19	NA		164	48	30	7	0.5	0.0	23.8	16.6	29	4	
Kali	4.9	3.8	112	8	0.5	0.6	62	28	15	7	0.2	0.1	6.3	1.1	21	5	
Zuari	4.2	4.4	101	11	NA		233	189	41	30	0.5	0.1	15.9	9.9	37	15	
Mandovi	3.1	4.9	115	16	0.8	1.1	90	31	20	7	0.2	0.2	15.6	17.2	24	9	
Northwest																	
Tapti	12.8	10.2	219	154	44.2	35.1	2925	3366	2104	2109	2.0	0.4	44.2	18.2	37	--	
Narmada	15.6	12.1	188	105	22.7	22.5	1041	592	334	355	0.4	0.1	37.7	17.6	39	17	
Mahisagar	6.8	7.9	285	115	12.5	18.6	754	880	151	192	0.5	0.5	39.0	12.4	33	21	
Wet upper overall mean																	
Wet estuary overall mean																	

318

319 **Table 3.** Variability of Salinity, Dissolved Silicon (DSi), Amorphous silica (ASi), Lithogenic silica (LSi), Total  
320 Suspended Matter (TSM), fucoxanthin, Dissolved inorganic Nitrogen (DIN) and Particulate Organic Carbon  
321 (POC) in the estuaries during the wet period. NA indicates non-availability of data

322

### 323 3.1.2. ASi

324

325 The ASi concentration ranges between 0.07 and 80 µM (Appendix A for individual samples, Tables 2 and 3 for  
326 average values). Unlike DSi, ASi is significantly variable between seasons ( $p < 0.001$ ) at large spatial scale, with  
327 lower average ASi during the dry period ( $4.2 \pm 6.3$  µM) than during the wet period ( $15.3 \pm 20.2$  µM). During the  
328 dry period, the eastern estuaries show significantly higher ASi ( $5.6 \pm 7.8$  µM) compared to the western estuaries

329 (2.2 ± 2.3 μM) (p<0.001). No such significant difference is observed between east (16.4 ± 17.6 μM) and west  
330 (14 ± 22 μM) flowing estuaries during the wet period.

331

332 Phytoliths were not counted to assess their contribution to the ASi pool; however some particle samples  
333 collected in Krishna (SE) and Rushikulya (NE) estuaries (where there was a large salinity gradient during dry  
334 and wet periods), were examined under SEM (Scanning Electron Microscope) analysis in order to look at the  
335 composition of biogenic material. This confirmed a predominant presence of healthy diatom cells during the dry  
336 period and fragmented diatom cells along with clay mineral components during the wet period (not shown).

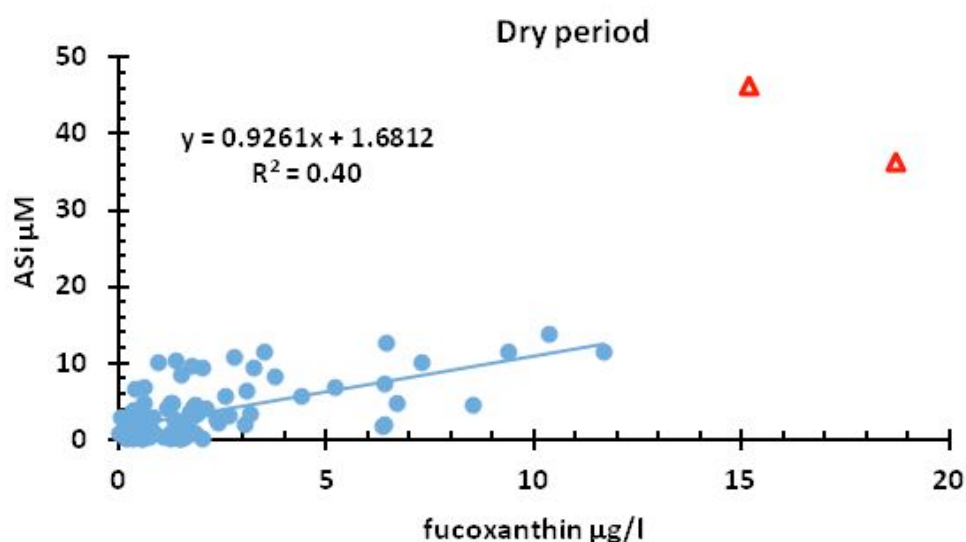
337

### 338 3.1.3. Fucoxanthin

339

340 Fucoxanthin is a diatom marker pigment, and its average concentrations in Indian estuaries are 1.86 ± 2.81 and  
341 0.56 ± 0.5 μg/l during the dry and wet periods respectively (Tables 2 and 3). During the dry period, there is a  
342 significant positive relation between ASi and fucoxanthin ( $R^2=0.40$  n=102, excluding 2 high ASi outliers, Fig.  
343 2) indicating that diatoms play a major role in ASi contents. However, only 40% of the ASi variability can be  
344 explained by the fucoxanthin, i.e. diatoms. No such positive relationship is noticed during wet season.

345



346

347 **Fig. 2** Best linear fit of ASi vs. fucoxanthin, to calculate the missing ASi. Two outliers (red triangles) from the  
348 small estuary Ponnaiyar (SE estuary) are excluded from the regression due to their very high ASi  
349 concentrations. Note that the regression line equation is used to recalculate the missing and negative ASi  
350 concentrations of the dry season for the PCA (see text).

351

### 352 3.1.4 LSi (Lithogenic silicon) and Total Suspended Material (TSM)

353

354 The average concentrations of LSi are 143 ± 343 μM and 720 ± 743 μM during dry and wet periods  
355 respectively. LSi is found to be particularly high in some estuaries, especially in the northern estuaries Haldia  
356 (NE), Tapti and Sabarmathi (NW) even during the dry period (Table 2 and Appendix A). Other than that, LSi is

357 higher during the wet period than during dry period in all the estuaries (Table 3). Unlike ASi and DSi which  
358 vary significantly between seasons and location (east or west coast), no such difference is shown on LSi (p=  
359 0.27 and 0.16 for the dry and wet periods respectively).

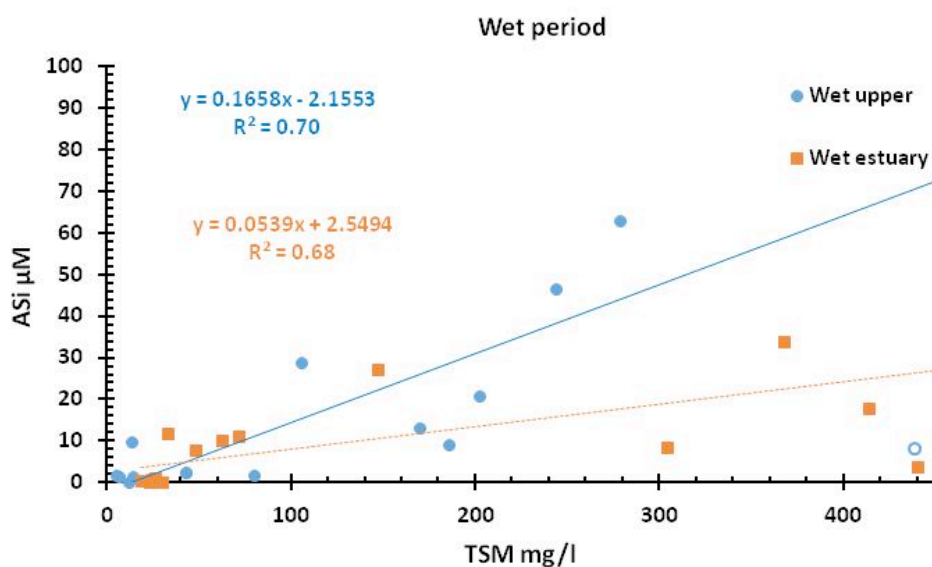
360

361 TSM is highly variable within each estuary across the salinity gradient (Tables 2 and 3) as well as for the dry  
362 ( $53 \pm 87$  mg/l) and wet ( $302 \pm 774$  mg/l) periods. 95% and 60% of all samples have less than or equal to 100  
363 mg/l of TSM during the dry and wet periods respectively. In most of the estuaries, in the dry period (80% of the  
364 samples), TSM is of moderate concentration (50-60 mg/l) with significant contribution of chl-a (not shown) and  
365 fucoxanthin, suggesting that turbidity may not act as a hurdle for the diatoms to grow as already discussed in  
366 Sarma et al. (2012). In contrast, a positive relationship is observed between TSM and discharge in Indian  
367 estuaries during the wet period ( $R^2=0.78$ ,  $n=11$ , excluding 2 estuaries), which confirms earlier findings in the  
368 Indian estuaries (Sarma et al., 2014). Haldia and Tapti estuaries are excluded from this relation because of their  
369 very low discharge and high TSM concentration (for Tapti) and vice versa (for Haldia). This is counterintuitive  
370 and may be due to the use of recalculated discharge data (10 years' average contribution, as described above)  
371 instead of the actual data at the time of sampling.

372

373 During the wet period, there is a significant positive relationship between TSM vs. ASi ( $R^2=0.45$ ,  $n=34$ ) and  
374 TSM vs. LSi ( $R^2=0.86$ ,  $n=49$ ) indicating the control of particulate Si supply via discharge. However, this TSM  
375 vs. ASi relationship is stronger when split into upper ( $R^2 = 0.70$ ) and lower ( $R^2 = 0.68$ ) estuaries respectively  
376 (Fig. 3). In addition, there is a significant positive relation between TSM and total particulate Si (ASi+LSi,  
377  $R^2=0.71$ , not shown) indicating that total particulate Si is mainly influenced by TSM. During the dry season,  
378 there is no significant relationship between ASi and TSM. However, a significant positive relationship exists  
379 between TSM vs. total particulate Si (ASi+LSi;  $R^2=0.40$ ,  $n=146$ ) and TSM vs. LSi ( $R^2=0.60$ ,  $n=146$ , excluding  
380 two outliers) indicating that the particulate Si pool is mainly controlled by lithogenic contribution in the  
381 estuaries during the dry period but this is mostly due to the latter (LSi).

382



383

384 **Fig. 3:** Best linear fit between ASi and TSM for wet season (circles: upper wet; squares: lower wet). TSM value  
 385 of estuary Haldia (NE, station 1, blue open circle) is excluded from the regression of the wet period upper  
 386 estuaries. Similarly, for lower estuaries, the best fit between ASi and TSM (closed boxes). Data for the estuary  
 387 Tapti (NW, station 3) was excluded from the regression because its TSM concentration exceeds average by more  
 388 than one order of magnitude (3572 mg/l) and is not shown in the graph. Note that the regression line equations  
 389 are used to recalculate the missing and negative ASi concentrations of the wet season for the PCA (see text).

390

### 391 3.1.5. DIN and POC

392

393 The average DIN distribution of Indian estuaries varies between  $14.1 \pm 15.2 \mu\text{M}$  and  $28.5 \pm 20.1 \mu\text{M}$  during the  
 394 dry and wet periods respectively (Tables 2 and 3) with significant seasonal differences. Similarly, the average  
 395 POC of Indian estuaries varies between  $94.4 \pm 93.7 \mu\text{M}$  and  $51.8 \pm 37 \mu\text{M}$  during the dry and wet periods  
 396 respectively, again with significant seasonal differences. A significant positive relation between TSM vs. POC  
 397 ( $R^2=0.43$ ,  $n=42$ ) and TSM vs. DIN ( $R^2=0.13$ ,  $n=50$ ), indicating POC and DIN have a terrestrial supply origin  
 398 and are related to lithogenic processes (more strongly by POC than DIN), will be treated below, when detailing  
 399 the PCA results.

400

### 401 3.2. Inter-estuary variability

402

403 In order to investigate the pattern of variability of the biogeochemical parameters among the different estuaries,  
 404 we apply, as explained in § 2.4, PCA to the seasonal data, followed by clustering of PCA results in the two  
 405 salinity categories  $<5$  and  $>5$  salinity. Results are shown in Table 4. In the upper estuarine region, three PCs are  
 406 identified explaining a total variance of 78% in the dry season and two PCs that explain 70% of total variance in  
 407 the wet season. In the lower estuarine region, the numbers of axes for dry and wet seasons are 3 and 2 PCs,  
 408 respectively, explaining 77-78% of the variability.

409

Variables	Upper -dry (n=22), sal<5			lower -dry (n=21), sal >5			Upper -wet (n=13), sal<5		Lower -wet (n=11), sal>5	
	PC 1 (33%)	PC 2 (25%)	PC 3 (20%)	PC 1 (34%)	PC 2 (27%)	PC 3 (17%)	PC 1 (50%)	PC 2 (20%)	PC 1 (58%)	PC 2 (19%)
Salinity	0.05	-0.42	<b>0.73</b>	0.22	-0.28	<b>0.82</b>	-0.10	<b>-0.62</b>	<b>0.62</b>	0.01
DSi	-0.22	<b>0.73</b>	-0.03	<b>0.62</b>	0.37	<b>-0.48</b>	-0.09	<b>0.82</b>	<b>0.64</b>	<b>-0.76</b>
TSM	<b>0.88</b>	-0.30	-0.03	<b>0.66</b>	<b>-0.46</b>	0.24	<b>0.94</b>	-0.20	<b>0.91</b>	-0.01
POC	<b>0.83</b>	-0.02	-0.16	<b>0.65</b>	0.25	-0.31	<b>0.93</b>	-0.08	0.35	<b>0.86</b>
DIN	0.05	0.01	<b>-0.89</b>	<b>0.58</b>	<b>-0.60</b>	-0.13	<b>0.81</b>	0.16	<b>0.89</b>	-0.13
ASi	<b>0.47</b>	<b>0.70</b>	<b>0.48</b>	<b>0.47</b>	<b>0.82</b>	0.2	<b>0.83</b>	0.29	<b>0.92</b>	0.00
LSi	<b>0.90</b>	-0.05	-0.07	<b>0.78</b>	<b>-0.44</b>	-0.09	<b>0.95</b>	-0.15	<b>0.93</b>	0.00
FuCo	0.22	<b>0.85</b>	0	<b>0.45</b>	<b>0.64</b>	0.49	0.06	<b>0.62</b>	<b>0.62</b>	0.47

410

411 **Table 4.** Correlation coefficient ( $r$ ) between PC axes and variables for the dry and wet periods. The values in  
 412 bold are significant at  $p<0.05$  level.

413

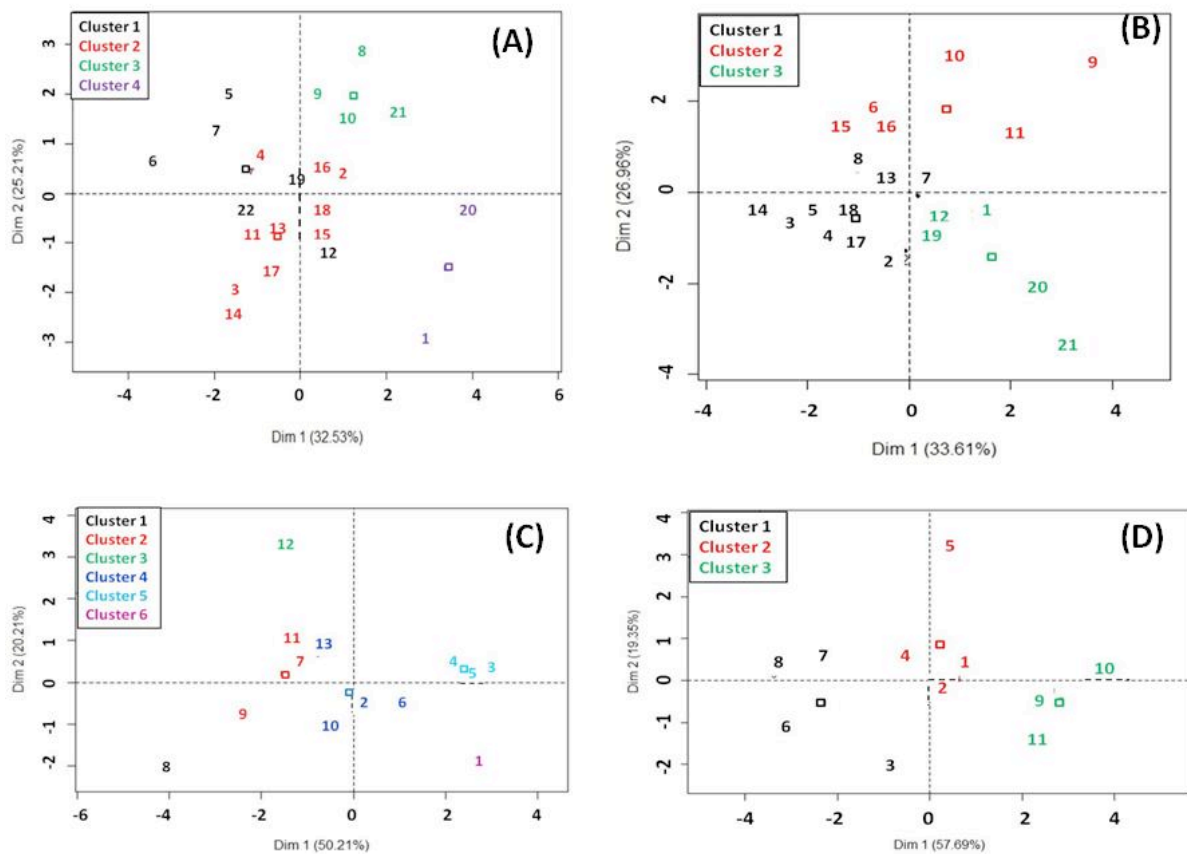
#### 414 3.2.1 - Dry period

415

##### 416 Upper estuaries

417 From the results shown in Table 4, PC1 is strongly related to the parameters ASi, POC, TSM and LSi, in  
 418 increasing order. Therefore, estuaries falling on the positive side of PC1 are dominated by lithogenic processes

419 such as weathering and erosion as a first order (primary) control (Fig. B1). In contrast, PC2 is primarily  
 420 influenced by biogenic parameters (ASi, fucoxanthin) and the estuaries falling under this axis might be  
 421 controlled by diatom production as a second order control. The influence of salinity and DIN is well pronounced  
 422 in the third axis (explaining 20% of variability), therefore representing only a third order control. Based on the  
 423 PCA results, clusters of estuaries from different geographic locations are identified (Fig 4A). The dominant  
 424 variables of each cluster are described in Table 5A. The complete dataset for all categories used for this  
 425 ordination technique are provided as tables in Appendix B.



426  
 427  
 428 **Fig. 4:** Factor map describing the clusters of samples on the Principal Component axes. Individual sample  
 429 names can be identified by their # provided in Table 5 which differ for each panel. A: Upper estuaries, dry  
 430 period. B: Lower estuaries, dry period. C: Upper estuaries, wet period. D: Lower estuaries, wet period.

431  
 432  
 433  
 434



5A- Upper estuaries - dry period							5B- Lower estuaries - dry period							
Estuaries	characterized variable	cluster mean	SD	Overall mean	SD	ratio <sub>(mean)</sub>	Estuaries	characterized variable	cluster mean	SD	overall mean	SD	ratio <sub>(mean)</sub>	
Cluster 1	NE: Nag (5), SE: Pen (7), Kris (6), Vai (12); NW: Nar (19), Mahi (22).	DIN	38	33	20	21	1.9	NE: Bai (2) Maha (3), Rus (4), Vam (5); SE: Pen (8), Kris (7); SW: KBW (13), Cha (14), Zua (17), Man (18).	ASi	2.1	1.2	4.2	5.5	0.5
		TSM	25	31	57	68	0.4		LSi	57	55	288	655	0.2
		Sal	0.4	0.2	1.7	1.4	0.2		DSi	63	24	96	51	0.7
Cluster 2	NE: Sub (2) Maha (3), Vam (4); SE: Amb (11); SW: KBW (13), Cha (14), Bha (15), Net (16), Kali (17), Zua (18).	Sal	2.5	1.2	1.7	1.4	1.5	NE: Nag (6); SE: Pon (9), Cau (10), Vel (11); SW: Bha (15), Net (16).	ASi	9.8	8.1	4.2	5.5	2.3
		DSi	152	107	219	132	0.7		Fuco	4.5	4.1	2.2	2.8	2.1
		DIN	9	6	20	21	0.5		POC	127	57	93	56	1.4
Cluster 3	SE: Pon (8), Cau (9), Vel (10); NW: Sab (21).	Fuco	5.03	1.56	1.76	1.87	2.9	NE: Hal (1); SE: Vai (12); NW: Nar (19), Tap (20), Sab (21).	DIN	38	19	15	16	2.5
		ASi	8.07	3.48	3.54	2.92	2.3		LSi	1168	1190	288	655	4.1
Cluster 4	NE: Hal (1) and NW: Tap (20)	DSi	358	141	219	132	1.6	TSM	123	141	54	69	2.3	
		POC	587	465	138	196	4.3	No cluster						
		LSi	1026	359	220	386	4.7							
		TSM	247	58	57	68	4.3							
5C- Upper estuaries - Wet period							5D - Lower estuaries- Wet period							
Cluster 1	SW: Kali (8)	DIN	5.4	0	27	14	0.2	NE: Rus (3); SW: Kali (6), Man (7), Zua (8).	DIN	7.5	5.3	22	19	0.3
									TSM	25	4	197	212	0.1
										LSi	109	28	944	1156
Cluster 2	SW: Net (7), Man (9); NW: Nar (11).	NULL					NE: Hal (1), Sub (2), Maha (4); SW: KBW (5).	NULL						
Cluster 3	NW: Tap (12)	Fuco	1.7	0	0.5	0.4	3.7	NW: Nar (9), Tap (10), Mahi (11).	TSM	465	118	197	212	2.4
		DSi	443	0	193	109	2.3		DSi	152	9	119	28	1.3
Cluster 4	NE: Sub (2); SW: KBW (6), Zua (10); NW: Mahi (13)	NULL					NE: Hal (1); SE: Vai (12); NW: Nar (19), Tap (20), Sab (21).	No cluster						
Cluster 5	NE: Rus (3), Maha (4); SE: God (5).	ASi	39	21	13	18	3.0							
		LSi	1594	357	691	780	2.3							
Cluster 6	NE: Hal (1)	TSM	229	43	125	172	1.8							
		NULL												

435

436 **Table 5:** Clustering results on samples (acronyms of estuaries along with geographical location; samples #  
437 refer to those displayed in Fig. 4 and are different for each category) with characterized parameters of each  
438 cluster including their mean values, standard deviation (SD) and ratio of mean of the cluster to the overall  
439 mean for dry upper (ratio<sub>(mean)</sub>). LSi, DIN, POC, ASi, DSi in  $\mu\text{M}$ ; TSM in mg/l and fucoxanthin in  $\mu\text{g/l}$ . A: Upper  
440 estuaries, dry season. B: Lower estuaries, dry period. C: Upper estuaries, wet period. D: Lower estuaries, wet  
441 period.

442

443 The estuaries of cluster 1 belong to eastern and northwestern regions and are dominated by high DIN (ratio<sub>(mean)</sub>  
444 greater than >1) and lower TSM and salinity (ratio<sub>(mean)</sub> <1). Cluster 2 mainly consists of estuaries from eastern  
445 and southwestern locations which are characterized by higher salinity and relatively less DSi and DIN  
446 concentrations compared to the mean upper dry (Table 5A). Cluster 3 mainly consists of southeast and  
447 Sabarmathi (NW) estuaries characterised by high fucoxanthin, ASi and DSi, showing no association with  
448 lithogenic variable. Cluster 4 consists of northern estuaries (Haldia and Tapti) and is highly controlled by  
449 lithogenic parameters with POC, LSi and TSM with ratio<sub>(mean)</sub> >>1 (Table 5A).

450

#### 451 Lower estuaries

452 PC1 and PC2, with strong associations of POC, TSM and LSi (34%) and fucoxanthin, ASi and DIN (27%), can  
453 clearly be considered as the signature of non-biogenic and biogenic processes respectively. PC3 (17%) with  
454 strong association for salinity represents the mixing of seawater (Table 4). The combined PCA and cluster  
455 analysis for lower estuaries allows for the distinction of three clusters (Fig. 4B).

456

457 The estuaries of cluster 1 (10 out of 21 estuaries) are from all regions except northwest, and are characterized by  
458 low ASi, LSi, POC and DSi (Table 5B). Estuaries from cluster 2 are all from eastern regions. Cluster 3  
459 comprises the eastern and northwestern estuaries. This cluster is mainly characterized by higher LSi, TSM and  
460 DIN concentrations (Table 5B).

461

### 462 **3.2.2 Wet period**

463

#### 464 *Upper estuary*

465 The overall variability and the significant correlation of the biogeochemical parameters to the PC axis are  
466 depicted in the Table 4 and Fig. B5. In total, 70% of the variability is explained by the first two axes (PC1 and  
467 PC2). The strong positive relations of DIN, ASi, POC, TSM and LSi parameters with axis 1 clearly shows that  
468 monsoonal discharge supplies a huge quantity of TSM along with weathered products (secondary and primary  
469 minerals) as well as organic plant materials. PC2 exhibits strong positive correlation with DSi and fucoxanthin  
470 and negative correlation with salinity (Table 4). Based on the PCA results, clusters of estuaries from different  
471 geographic locations in the case of upper estuary are identified (Fig. 4C). The dominant variables of each cluster  
472 are described in Table 5C. The complete dataset for all categories used for the ordination technique are provided  
473 as tables in Appendix B.

474

475 In cluster 1, DIN is the unique characteristic variable with 80% lower concentration than the overall mean of the  
476 category. The upper Khali estuary was sampled for the wet season from the shore around a mangrove area,  
477 which might explain these data particulars.

478

479 Cluster 3 (only Tapti in NW) is mainly characterized by higher DSi and fucoxanthin (Table 5C). Together with  
480 high ASi (9.8  $\mu\text{M}$ ), even though not different from the category mean, this indicates the possible signature for  
481 diatom occurrence. This suggests a relatively minor lithogenic impact compared to that in other clusters.

482

483 Interestingly, there is no significant characteristic variable governing the estuaries of cluster 2 (three estuaries  
484 from western regions) and cluster 4 (four estuaries from northeast and western regions). This means that none of  
485 the variables are significantly different from the overall mean and that they can thus be considered as  
486 representative of the average upper wet estuaries. The estuaries of these two clusters are relatively close to one  
487 another on the factor map (Fig. 4C). Cluster 6 also represents a single estuary (Haldia, NE), but this estuary is  
488 quite remote from the location of the estuaries of clusters 2 and 4. Notably, Haldia is linked to the Ganges-  
489 Brahmaputra system, which is known to behave differently from the other Indian rivers due to its more  
490 perennial supply of freshwater. Finally, cluster 5 includes only estuaries from the eastern region. These estuaries  
491 are characterized by high TSM, LSi and ASi (Table 5C).

492

#### 493 *Lower estuary*

494 In total, 77% of variability is explained by PC1 and PC2 (Table 4 and Fig. B6). PC1 alone explains 58% of  
495 variability with strong relationships with salinity, LSi, TSM, DIN, ASi, and fucoxanthin towards the positive  
496 end of the axis (Table 4). The remaining 19 % is explained by PC2 with strong relationship of DSi towards  
497 negative and POC towards positive end of the PC2 axis. The suspended material via river runoff is naturally  
498 considered to be the dominant controlling mechanism for LSi, ASi, and TSM source to the estuaries in high  
499 discharge season, though there is significant influence of salinity, i.e. mixing with seawater.

500

501 The clustering of PCA results (Fig. 4D and Table 5D) reveals clustering of estuaries from northeast and  
502 southwest regions (cluster 1), estuaries from the same regions but not included in cluster 1 (cluster 2) and the  
503 three estuaries from NW (cluster 3). Cluster 2 is similar to some upper estuary clusters and has no characteristic  
504 biogeochemical variable.

505

## 506 **4. Discussion**

507

### 508 **4.1 Biogeochemistry of the Si pools**

509

#### 510 *4.1.1 Comparison with previous Si data in rivers*

511

512 The ASi values observed in the Indian estuaries are within the range of world estuaries and comparable with  
513 other tropical estuaries (Table 6). Weathering and erosion via terrigenous supply played a dominant role on the  
514 particulate Si pool, including ASi, during the wet period. A similar observation was made for the river Huanghe,  
515 China, where high erosion of topsoils is responsible for higher ASi supply (Ran et al., 2015). Higher DSi  
516 content in the eastern estuaries, compared to the western estuaries, may be explained by different soil-water  
517 interaction times during which silicon leached, as observed for other tropical rivers such as Tana in Kenya  
518 (Dunne, 1978; Hughes et al., 2012). The east coast Indian estuaries belong to larger watersheds, with wider  
519 plains and longer residence times of soil-water interaction, compared to the west coast estuaries with smaller  
520 watershed and steeper slopes (Nayak and Hanamgond, 2010).

521

522 Before reaching the coastal water, the DSi concentrations in estuaries are altered through several mechanisms -  
523 dilution with seawater, biological uptake, sediment settling, dissolution or adsorption - desorption (Struyf et al.,  
524 2005; Zhu et al., 2009; Lehtimäki, et al., 2013; Lu, et al., 2013; Carbonnel et al., 2013; Raimonet et al., 2013).  
525 In the present study, the observed DSi concentration of the upper estuaries are similar to those reported earlier  
526 for Indian rivers (Sarma et al., 2009; Gurumurthy et al., 2012; Meunier et al., 2015; Frings et al., 2015) and  
527 other tropical rivers (Liu et al., 2009; Hughes et al., 2011, 2012, 2013; Ran et al., 2015). The abundance of  
528 diatoms in the Si pool is consistent with the share of diatoms in the total phytoplankton counts of  $61 \pm 26\%$   
529 among the estuaries during dry period (Durgabharathi, 2014).

530

531 The calculated contribution of ASi to the mobile Si pool ( $ASi/(ASi+DSi)$ ) shows higher ASi contribution during  
532 wet season ( $8.8 \pm 10\%$ ) compared to dry season ( $3.5 \pm 5\%$ ). The results are lower than those of the other world  
533 river systems (16%; Conley, 1997) and Huanghe River (65% during high flow; Ran et al., 2015) but comparable  
534 to the tropical systems such as river Congo (6%; Hughes et al., 2011) and slightly higher than those observed for  
535 the Amazon basin (3%; Hughes et al., 2013).

536

<i>River/estuary</i>	<i>ASi <math>\mu\text{mol/l}</math> -range</i>	<i>References</i>
<i>Tropical</i>		
Huanghe river	16-285	<i>Ran et al., 2015</i>
Nyong basin river	0.4-1.2	<i>Cary et al., 2005</i>
Congo river	0.9-40	<i>Hughes et al., 2011</i>
Amazon river	<DL-13.4	<i>Hughes et al., 2013</i>
Changjiang river	0.5-4.0	<i>Cao et al., 2013</i>
Lake malawi (Shire River outflow)	2.9-69	<i>Bootsma et al., 2003</i>
Ganges	<DL to 300	<i>Frings et al., 2014</i>
Youngjiang	1.7	<i>Liu et al., 2005</i>
Indian estuaries-upstream-dry	0.1-36	<i>present study</i>
Indian estuaries - upstream wet	0.2-63	<i>present study</i>
<i>Subtropical</i>		
Estuary of Taiwan	5-6.1	<i>Wu, et al., 2003</i>
<i>Temperate</i>		
Scheldt estuary	7.0-81	<i>Carbonnel et al., 2013</i>
Baltic sea catchments	0-100	<i>Humborg et al., 2006</i>
Oder river	10-100	<i>Sun et al., 2013</i>
Mississippi river USA	14.1	<i>Conley. 1997</i>
Daugava river	1.0-12	<i>Aigars et al., 2014</i>
Rhine river	1.4-5.9	<i>Admiraal et al., 1990</i>
Vantaa river estuary	11-192	<i>Lehtimäki et al., 2013</i>
<i>Polar</i>		
Lena river	4.0-17	<i>Heiskanen et al., 1996</i>

537

538 **Table 6.** *ASi or BSi distribution in world rivers/estuaries, including the present study upper estuaries.*

539

540 The variability of LSi in Indian estuaries is comparable to that of the Aulne estuary (56-573  $\mu\text{M}$ ) in France  
541 (Ragueneau et al., 2005) and the tropical Changjiang estuary ( $560 \pm 1410 \mu\text{M}$ ) in China (Lu et al., 2013). It is in  
542 accordance with previous studies in the Godavari estuary (Sarma et al., 2009, 2014). The results from the Haldia  
543 estuary ( $566 \pm 272 \text{ mg/l}$ ) and other Indian estuaries are found to be in the range of Ganges and comparable with  
544 other European estuaries, despite largely varying TSM concentrations in the former (49 to 2000  $\text{mg/l}$  at surface;  
545 Frings et al., 2014) and in the latter (a few  $\text{mg/l}$  to few  $\text{g/l}$ ; Middelburg and Herman, 2007).

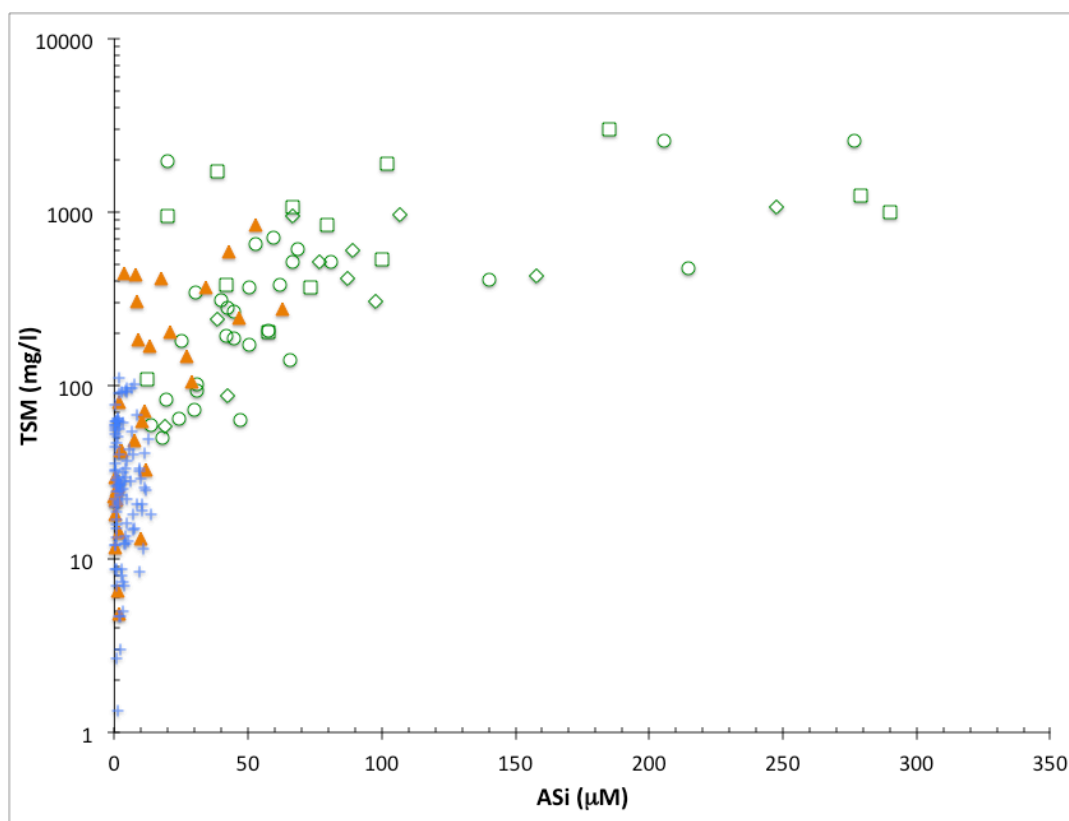
546

547 *4.1.2 Comparison with previous ASi data in Indian rivers*

548

549 The only previous study on ASi in the Ganges river of the Indian subcontinent showed ASi is highly variable  
550 (from below detection limit to  $> 300 \mu\text{M}$ ) and its origin cannot be explained by biogenic causes only (Frings et  
551 al., 2014). Our results confirm these findings. Compared to that of the Ganges basin, the ASi and TSM  
552 variabilities in other major and minor estuaries observed in this study, are lower.. The concentrations of  
553 suspended matter (50  $\text{mg/l}$  to several  $\text{g/l}$ ) and ASi (ranging from below detection limit to up to  $300 \mu\text{M}$ ) in  
554 Ganges are often several times higher compared to our data from other Indian estuaries (e.g. average for wet  
555 upper estuaries:  $11 \pm 15 \mu\text{M}$  for ASi and  $123 \pm 200 \text{ mg/l}$  for TSM, cf. Table 1). Comparing both studies is not  
556 trivial, for several reasons. (i) The Frings et al. (2014) study dealt with a single one of India's largest river  
557 basins, Ganges, whereas the present study surveys several estuaries with a wide range of sizes. (ii) Unlike other  
558 rivers in India (monsoonal rivers), the Ganges basin is a perennial river with relatively low seasonal variability

559 on its discharge and is characterized by particularly high TSM due to high erosion of the Himalayan mountains.  
 560 (iii) There might be a methodological issue on ASi measurement as Frings et al. (2014) used a 1% Na<sub>2</sub>CO<sub>3</sub>  
 561 leaching (Clymans et al., 2011) while the current study uses 0.2 M NaOH (Ragueneau et al., 2005). This  
 562 Na<sub>2</sub>CO<sub>3</sub> method was found to potentially overestimate ASi, whereas the use of the strong NaOH base may  
 563 underestimate ASi (Barao et al., 2015). Although the ASi values of the present study are several times lower  
 564 than the mean ASi (68 μM) of Ganges, the relationship between TSM and ASi of our data set follows the same  
 565 logarithmic trend as Frings et al., 2014 for surface waters (Fig. 5). Indeed, our upper wet estuaries TSM versus  
 566 ASi variability is consistent with the trend of Frings et al. (2014) as our average TSM is 125 mg/l (Table 2).  
 567 According to the Ganges TSM – ASi relationship, this should correspond to 12-40 μM ASi (Fig. 5) and we find  
 568 12 μM (Table 2). Hence, we can be confident there is no methodology issue in our ASi estimates since the  
 569 orders of magnitude in both studies are consistent and the relatively lower TSM we find in our Indian estuaries  
 570 can explain our lower ASi compared to those from Ganges, (Fig. 5).  
 571



572  
 573 **Fig. 5** Comparison of TSM vs. ASi in Ganges river (green circles: surface; green diamonds: mid-depths; green  
 574 squares: deep samples; data from Frings et al., 2014) and Indian estuaries (orange triangles: wet season; blue  
 575 crosses: dry season; this study).  
 576

577 **4.2. Si:N ratios and coastal eutrophication potential**

578  
 579 In all estuaries, the DSi:DIN ratios are much higher than the “Redfield-Brzezinski ratio” needed for diatoms  
 580 which is ~1 under non-limiting conditions (Brzezinski, 1985): for the upper estuaries, the average Si:N ratios are  
 581 9.8 (range of 1.4 – 25, excluding one outlier at > 400) and 23 (range of 2.3 - 155) during wet and dry seasons,

582 respectively. The average Si:N ratios of the highest salinity samples is 12 (range of 1.5 – 85) for both wet and  
583 dry seasons. Hence, whatever the season, either in the freshwater end-member (i.e. supply to estuaries) or higher  
584 saline samples (i.e. supply to the coastal North Indian Ocean), Si is never limiting relative to N. Consequently,  
585 the Indicators for Coastal Eutrophication Potential (ICEP) which “represent the new production of non-siliceous  
586 algal biomass potentially sustained in the receiving coastal water body by either nitrogen (...) delivered in excess  
587 over silica” (Garnier et al. 2010) will all be negative, meaning that coastal eutrophication should not take place  
588 around the mouth of our studied estuaries. Whether this explains why coastal Indian waters rarely face  
589 eutrophication and/or whether such absence of eutrophication is due to strong coastal currents inducing quick  
590 dilution and/or high turbidity (Rao and Sarma, 2013; Krishna et al., 2016) remains to be confirmed, but clearly,  
591 high silicon supply to the coast, even downstream the estuarine filter, is likely to play a significant role. Sarma  
592 et al. (2013) observe Si:N ratios mostly above 1 along the coastal Bay of Bengal and attribute them to high  
593 supply of Si from rivers. Noteworthy, we do not observe seasonal variation of DSi:DIN ratios of the estuarine  
594 supply to the coast.

595

### 596 **4.3. Inter-estuary biogeochemical processes**

597

598 Apart from seasonal variability in biogeochemical processes, the distinct functioning of each estuary is also  
599 determined by non-seasonal features such as geographical location (climate), topography (e.g., larger watershed  
600 size and smoother slopes in the east) and land-use practices (e.g., type of agriculture, urbanization etc.). All  
601 these properties affect runoff and biogeochemical characteristics making it hard to isolate the processes  
602 controlling the variability occurring in estuaries by looking at the whole dataset using only regional averages as  
603 discussed above. Principal Component Analysis allows for better inter-comparison of the samples and will  
604 identify the parameters explaining variability in concentrations of ASi, LSi and DSi, independently of the region  
605 of sampling (e.g. Xue et al., 2011).

606

#### 607 **4.3.1. Dry Period**

608

##### 609 *Upper estuary*

610 Cluster 1, characterized by high DIN, suggests more supply of nitrogen via artificial fertilizer usage, which is  
611 especially true for the northern estuaries. The anthropogenic activities such as supply of domestic waste,  
612 agriculture and industrial activity are likely responsible for the higher, dominating DIN in these estuaries (150  
613 kg/ha fertilizer usage in Gujarat-NW region compared to other western states like Kerala, 113 kg/h, and  
614 Maharashtra 134 kg/h — Ministry of agriculture, 2012-2013). This confirms the higher impact of fertilizer  
615 usage in the northern estuaries reported by Sarma et al. (2014), using nitrogen isotopes.

616

617 Cluster 2 mainly consists of estuaries from northeastern and southwestern locations characterized by higher  
618 salinity and relatively lower DSi and DIN concentrations compared to the mean upper dry (Table 5). This  
619 suggests that the seawater intrusion and low fresh water supply could be responsible for low DSi and DIN.  
620 Higher tidal amplitude in northern and smaller watersheds of southern estuaries favours more seawater  
621 characteristics and influences the biogeochemistry.

622

623 In the estuaries of cluster 3, high fucoxanthin and ASi indicate diatoms presence, while high DSi suggests the Si  
624 is coming from the dissolution/decomposition of biogenic material (e.g., dead diatoms or phytoliths) that have  
625 recently settled in the surface sediments. It is known that ASi dissolution at the sediment – water interface can  
626 be a significant supply of DSi in estuaries (Struyf et al., 2005; Delvaux et al., 2013; Raimonet et al., 2013). Our  
627 data do not allow quantifying such benthic flux, but we suggest that it should contribute significantly to the high  
628 DSi concentration in this cluster. Enhanced phytoplankton biomass associated with lower TSM was attributed  
629 with high in-situ production observed in the Indian estuaries (e.g. Godavari by Sarma et al., 2009; and Sarma et  
630 al., 2014). For cluster 4, with high lithogenic contents, erosion continuously supplies terrigenous material with  
631 high suspended material load to the upper estuaries.

632

633 Overall, in the dry upper category, we show that the estuarine biogeochemistry variability is strongly dominated  
634 by diatoms (cluster 3), lithogenic processes (cluster 4) and, partly dominated by seawater intrusion (cluster 2),  
635 and by a possible anthropogenic impact (cluster 1).

636

637 *Lower estuaries*

638 A combination of both biogenic (diatom uptake) and non-biogenic (lithogenic supply) processes explain the  
639 variability of Si parameters in the lower estuaries (Fig. 4B and Appendix B3). Though salinity explained 17%  
640 variability in PC3 of this category, none of the clusters were significantly controlled by salinity. Therefore the  
641 materials supplied from the upper estuaries may still be controlling the variability of LSi, TSM and DIN in these  
642 lower estuaries.

643

644 The estuaries of cluster 1 seem to be controlled by lithogenic processes, while the estuaries of cluster 2 support  
645 diatom production (higher ASi, fucoxanthin and POC and lower DIN) and three of these estuaries are in cluster  
646 3 of the upper estuaries category (especially the southeast estuaries). Thereby, higher diatom production is  
647 favoured throughout the length of these estuaries. The lower estuaries of cluster 3 are mainly controlled by  
648 terrestrial (non-biogenic) supply of materials. Excepting Vaigai, these estuaries are all from the north,  
649 characterised by higher tidal amplitude that could favour sediment resuspension (7 to 10m compared to 1 to 2m  
650 for most of the other; Sarma et al., 2014).

651

#### 652 **4.3.2. Wet period**

653

654 *Upper estuary*

655 The strong positive relations of the DIN, ASi, POC, TSM and LSi parameters on axis 1 clearly suggest that  
656 monsoonal discharge is responsible for the huge TSM supply along with weathered products (secondary and  
657 primary minerals) as well as organic plant materials. This high erosion is the main factor controlling the  
658 biogeochemical variables of the upper estuaries during the wet period. However, the lithogenic control of  
659 material supply is variable among the identified clusters, the variability depending on the climate, discharge and  
660 the time of sampling. Salinity (mixing) exerts a second-order control on DSi. The clustering of PCA results (Fig.

661 4C and Table 5C) distinguishes Khali (SW, cluster 1), Tapti (NW, 3) and Haldia (NE, 6) as single estuary  
662 clusters, distinct from the other estuaries.

663

664 The association in cluster 5 reveals that terrigenous material supply via monsoon discharge is the clear  
665 controlling mechanism of Si variability here. Further, the terrestrial supplies contain a high level of ASi not  
666 originating from live diatoms as this high ASi was not related to high fucoxanthin. The ASi pool may contain  
667 diatom debris (as observed on SEM samples from Rushikulya, not shown) along with phytoliths and lithogenic  
668 ASi. Indeed, there should be a common process relating ASi, LSi and TSM in this cluster as these three  
669 variables are higher by a similar enrichment factor (2-3) compared to the mean, the most likely responsible  
670 process being soil erosion.

671

672 *Lower estuary*

673 In cluster 1, the concentration of ASi, TSM, DIN and LSi are particularly lower than the mean (by -70 to -95%,  
674 Table 5D), and this indicates that most of the lithogenic supply from the upstream has settled and will not reach  
675 the coastal ocean. This was particularly obvious for Rushikulya which is characterized by very high TSM and  
676 LSi in the upper estuary during wet season as compared to the lower estuary. Estuaries in this cluster 1 are from  
677 relatively smaller watersheds with steeper slopes (for SW) and smaller plains (Table 1). This may explain higher  
678 settling once the high particle load enters the estuary.

679

680 The estuaries of cluster 3 are mainly controlled by lithogenic supply, as evidenced by the TSM and LSi  
681 concentrations which are ~2.5 folds higher than the overall mean of the category. The estuaries under this  
682 category are usually larger in size and the rivers run in wider plains with heavy runoff during monsoon period.  
683 The average TSM and LSi of cluster 3 is much higher than TSM and LSi measured in the same estuaries  
684 upstream, highlighting the non-conservativity of these parameters (Appendix A). Because of the larger size and  
685 longer length of these estuaries, it is possible that lithogenic supply from land surrounding the estuary is  
686 significant and contributes to an increase in the particle load. Moreover, for the NW estuaries (Tapti, Narmada),  
687 the watersheds are characterized by semi-arid climate and vegetation that should favour more erosion.  
688 Noteworthy, Narmada and Tapti are in cluster 3 (lower dry category), also characterized by high DIN, TSM and  
689 LSi. As already mentioned, the tidal amplitude of northern estuaries is the highest (Sarma et al. 2014) and  
690 sediment resuspension is likely to be higher. In any case, these estuaries are an important source of particles to  
691 the coastal ocean.

692

693 The cluster 2 estuaries have large ranges of LSi, TSM and ASi concentrations ( $759 \pm 592 \mu\text{M}$ ,  $168 \pm 168 \text{ mg/l}$   
694 and  $11.8 \pm 3.9 \mu\text{M}$  respectively) which are very similar to those of the upper mean wet estuaries and it seems  
695 likely that in this category particulate material supplied by freshwater source is efficiently transferred to the  
696 lower estuary with little modification.

697

698 Overall, the lower wet estuaries are mainly controlled by the lithogenic processes, which are however of  
699 variable origins and fate within this lithogenic material, namely (i) efficient sediment trapping within the lower



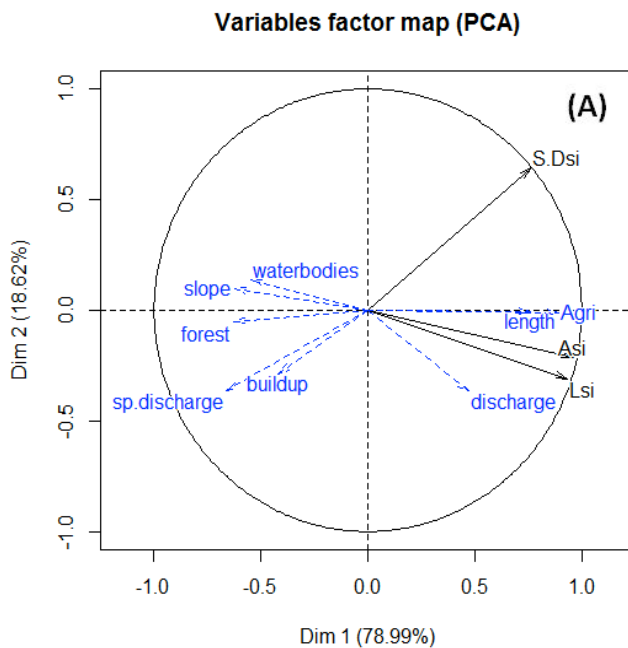
700 estuary (cluster 1), (ii) efficient transfer to the coastal ocean (cluster 2) and (iii) local input of lithogenic  
701 particles in the case of large estuarine watersheds (cluster 3).

702

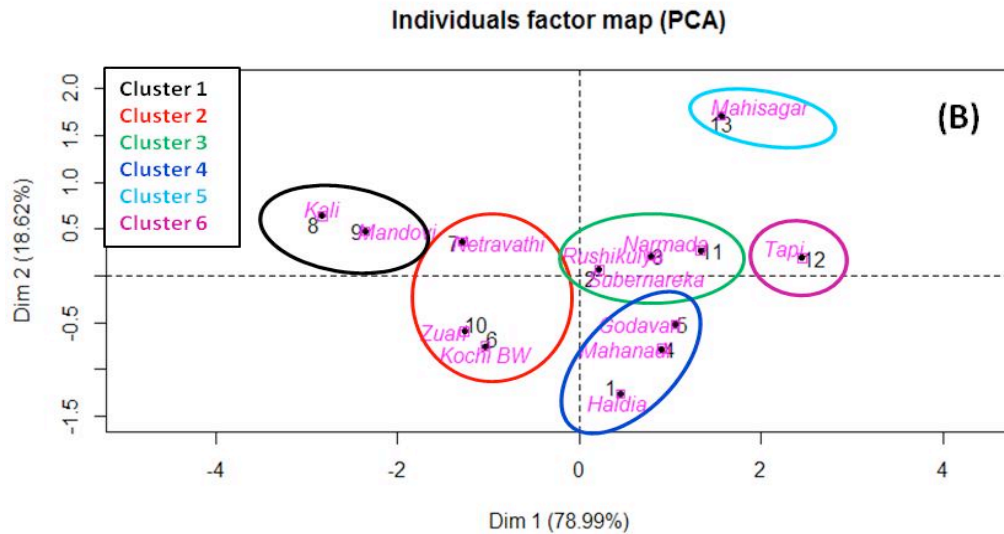
#### 703 4.4. Impact of land use on the Si cycle

704

705 India being an agricultural country with ~1.3 billion inhabitants, an attempt has been made to visualize the  
706 impact of land use (agriculture, forest cover, built-up lands, water bodies) and other general watershed  
707 characteristics on the Si cycle in the Indian estuaries since earlier studies did demonstrate anthropogenic impact  
708 on continental Si cycle (e.g. Humborg et al., 2006, Conley et al., 2008; Struyf et al., 2010). The PCA results are  
709 analysed to envisage relationships among the variables and the prevailing land-use pattern affecting the Indian  
710 estuaries. The impact of land use can be better evidenced by the terrestrial supply tightly associated with  
711 discharge during wet period. Therefore the impact of land use is studied only on the Si parameters (ASi, DSi and  
712 LSi) during wet period on the mean estuary (upper + lower). The land-use and watershed characteristics data  
713 were obtained from <http://www.india-wris.nrs.gov.in/>. Note that the NRSC-WRIS website provides regional  
714 averages for some adjacent watersheds of the same land-use pattern (Table 1). Contrary to PCA on all  
715 biogeochemical parameters, in this case the PC analysis is performed based only on the three Si parameters  
716 (DSi, ASi and LSi) and the watershed characteristics as supplementary variables to see how they correlated to  
717 the PC axes. In addition to land use, we include runoff, slope, discharge and length of the river (representative of  
718 watershed surface since both are highly correlated with  $R^2 = 0.8$ ).



719



720  
 721 **Fig. 6a and b**, PCA analysis on the impact of land use in the Indian estuaries during the wet period. A)  
 722 Relationship among the variables and b) Individual factor map and clustering with Indian estuaries based on  
 723 PCA results.

724  
 725 The PCA results explain 79% of the overall Si variability along the first axis and 19% variability along the  
 726 second axis. PC2 shows less variability (Eigen value <1) and no significant correlation with the variables can be  
 727 observed (Fig. 6a and Table 7). The three highest correlations on the positive side of PC1 are with ASi, LSi and  
 728 % agriculture ( $r$  close to 0.9) and, to a slightly lesser extent, for the length of the river and DSi ( $r=0.76$  each).  
 729 This is consistent with higher agricultural activity and the fact that larger watersheds have increased supply of  
 730 ASi and LSi while higher forest cover reduces soil erosion. Noteworthy is the fact that the northern estuaries  
 731 (NE and NW; clusters 3 to 6) tend towards the positive end of PC1, whereas the southern (SW, clusters 1 and 2)  
 732 estuaries tend towards the negative side of PC1. This could be explained by a relatively more extensive forest  
 733 cover (avg. 35%) in the SW region (Western Ghats) compared to other regions (avg. forest cover for the NE and  
 734 NW regions, 26%), preventing soil erosion. The SW rivers also have steeper slopes and less residence time of  
 735 water especially when runoff is high, reducing the Si supply to the coastal water relative to the other eastern and  
 736 northwestern estuaries. In contrast, the wider plains (longer watershed) and higher agriculture practice along the  
 737 eastern and northwestern regions (avg 60%) compared to SW region (avg 47%) favours more supply of land-  
 738 derived Si (via biogenic and lithogenic mechanisms) to the Bay of Bengal when compared to the Arabian Sea  
 739 (Fig. 6b). Undoubtedly, increasing urbanization (e.g. deforestation) can also alter the Si cycle and changes in the  
 740 Si supply to estuaries in the future, as shown in the case of estuaries elsewhere in the world (e.g. Humborg et al.,  
 741 2006; Conley et al., 2008; Laruelle et al., 2009; Delvaux et al., 2013; Xiangbin et al., 2015).

742

Variables	wet period (upper+lower)	
	PC 1 (77.9%)	PC 2 (17.8%)
ASi	<b>0.96</b>	-0.21
LSi	<b>0.93</b>	-0.30
DSi	<b>0.76</b>	0.64
Buildup	-0.42	-0.28
Agri	<b>0.89</b>	-0.01
Forest	<b>-0.63</b>	-0.05
Waterbodies	<b>-0.55</b>	0.14
length	<b>0.76</b>	0
Slope	<b>-0.62</b>	0.09
Discharge	0.47	-0.36
Runoff	<b>-0.66</b>	-0.37

743

744 *Table 7. Correlation of land use and Si variables on PC axis 1 and 2 during wet period.*

745

#### 746 **4.5 Fluxes of ASi, LSi and DSi to North Indian Ocean from Indian sub-continent**

747

748 Knowledge of riverine contributions of dissolved and particulate materials to the ocean is essential to understand  
749 the elemental fluxes and balances on a global scale. Taking the uncertainties on Si river fluxes to the ocean,  
750 especially in tropical environments (Tréguer & De La Rocha, 2013) into account, we calculate the total flux of  
751 DSi, ASi and LSi delivered by the upper estuaries to the North Indian Ocean. The Indian estuaries are mostly  
752 monsoonal estuaries and receive maximum runoff during the southwest monsoon period when most of the  
753 supply of materials via rivers also occurs (Subramanian et al., 2006). The wet season considered in this paper is  
754 the 4-month duration when  $76 \pm 10\%$  of annual discharge occurs in the estuaries (Table 1), and very high ASi  
755 and LSi concentrations are observed, compared to the dry season, even if DSi shows similar concentrations  
756 (Tables 2 and 3). Therefore, we calculate the material flux for the wet period as it should represent at least three-  
757 fourths of the annual Si flux. The flux is calculated by multiplying the wet season's discharge (Table 1) and the  
758 concentration of Si parameter of the upper estuaries and expressed as Gmol ( $10^{12}$  mol) for wet season.  
759 Uncertainties on these fluxes for each estuary are expressed in terms of (i) the standard deviation of wet  
760 season's discharge based on a 10 years average to take into account inter-annual variability of discharge, and (ii)  
761 the standard deviation of the mean upper wet ASi, DSi and LSi concentrations to take into account sampling  
762 variability. Where only one sample is available, we use the relative standard deviation of the closest estuary.

763

764 We estimate that the Indian monsoonal estuaries sampled in our study supply  $49 \pm 6$ ,  $3 \pm 1.6$ ,  $303 \pm 47$  Gmol of  
765 DSi, ASi and LSi respectively to the upper estuaries of Northern Indian Ocean during wet season. Of these  
766 quantities, 55% of DSi, 92% of ASi and 94% of LSi are supplied to the Bay of Bengal and the rest to the  
767 Arabian Sea (Table 8). It is interesting to note that the supply of DSi to the Arabian Sea and the Bay of Bengal  
768 are comparable, while the ASi and LSi supply were  $\sim 25$  and 10 times higher for the Bay of Bengal.

769

770 From the above discussion, ASi, LSi, DSi and TSM do not necessarily follow a conservative behaviour along  
771 salinity gradient, even during the wet season (Appendix A). Therefore, we correct the fluxes during wet season

772 to the upper estuaries for non-conservativity to obtain more relevant estimates for silicon fluxes to the coastal  
773 North Indian Ocean. Non-conservativity is estimated by recalculating the expected conservative concentration  
774 of the highest salinity sample available with respect to its measured concentration. We use coastal values (taken  
775 from literature) for the seawater end-member values and the lowest salinity station as fresh water end-member.  
776 Coastal seawater concentrations of DSi, ASi and LSi of 5µM, 2 µM, 5 µM, respectively, are taken from Gupta  
777 et al. (1997), Naqvi et al. (2010) and Sarma et al. (2013). The non-conservative fluxes do not modify the DSi  
778 fluxes much, because most of the DSi variability adheres to conservative mixing during wet season. However,  
779 this is not the case for NW estuaries which show a dramatic increase of particle supply along the salinity  
780 gradient. These calculations show that the estuaries sampled east of the Arabian Sea (AS) and west of the Bay of  
781 Bengal supply fluxes of the same order of magnitude to their respective seas (Table 8).

782

Estuaries	Bulk fluxes to upper estuaries						Net fluxes to Ocean (assuming non-conservativity)					
	DSi	SD	ASi	SD	LSi	SD	DSi	SD	ASi	SD	LSi	SD
	Gmol/wet season						Gmol/wet season					
Haldia*	4.3	0.4	0.22	0.11	85	7	5.7	0.5	0.5	0.27	77	6.8
Subarnarekha*	1.7	0.3	0.15	0.17	5	3	1.3	0.2	0.1	0.10	4	2.3
Mahanadi	7.5	1.7	NA		72	24	6.0	1.4	NA		64	21
Rushikulya	0.2	0.1	0.06	0.02	2	0.6	0.1	0.1	0.0	0.01	0.3	0
Godavari	13.3	4.0	2.02	1.62	121	39	12	3.5	0.6	0.47	94	30
Kochi BW	0.8	0.1	NA		2	2	1.0	0.1	NA		13	11
Netravathi	1.2	0.3	0.01	0.001	2	0.5	0.9	0.2	NA		3	0.9
Kali*	0.5	0.0	0.00	0.004	0.2	0.0	0.6	0.01	0.001	0.0007	0.4	0.1
Zuari*	0.3	0.0	NA		0.7	0.5	0.3	0.03	NA		0.6	0.4
Mandovi	0.3	0.1	0.00	0.001	0.2	0.1	0.3	0.1	0.0001	0.00004	0.6	0.2
Tapti	4.3	0.2	0.09	0.004	0.6	0.0	2.7	0.1	0.6	0.03	48	2
Narmada	11.2	3.0	0.09	0.02	10	3	14	3.7	1.1	0.30	217	59
Mahisagar	3.4	2.0	0.02	0.01	3	3	2.5	1.5	0.2	0.11	189	249
Bay of Bengal (BOB)	27	4.4	2.44	1.64	285	46	25	3.8	1.2	0.55	239	37
Arabian Sea (AS)	22	3.6	0.22	0.03	18	5	22	4.0	1.9	0.32	472	256
Total to north Indian Ocean	49	5.7	2.7	1.6	303	46	47	5.5	3.1	0.63	711	259
Extrapolating to total BoB							211	32	10.3	4.7	2028	317
Extrapolating to total AS							80	15	6.9	1.1	1717	932

783

784 **Table 8.** ASi, LSi, DSi and TSM fluxes of Indian estuaries draining into the Bay of Bengal and Arabian Sea  
785 during wet period with standard deviation estimates (SD). Fluxes to the left are calculated using upper wet  
786 concentrations. Fluxes to the right are estimates of fluxes to the coastal ocean, taking into account the non-  
787 conservativity of the variables along the salinity gradient (see text for details). For estuaries marked \*, 10 years  
788 average discharge data is unavailable, and the wet period contribution from annual mean discharge data  
789 reported in Krishna et al. (2016) is used instead. The adjacent estuaries % of wet period contribution is used to  
790 calculate the discharge of Haldia, Subarnareka, Kali and Zuari (i.e., Mahanadi wet period contribution was  
791 used for Haldia and Subarnareka; Netravathi was used for Kali and Mandovi for Zuari.)

792

793 Our results do not imply the total sediment supply to the Arabian Sea and the Bay of Bengal to be similar. It is  
794 well known that this is not the case, and the sediment supply to the entire Bay of Bengal is higher than the  
795 supply to the entire Arabian Sea (Nair et al., 1989; Ittekkot et al., 1991). The estuaries sampled in our study  
796 represent a discharge to the Arabian sea of  $82 \pm 12 \text{ km}^3$  which is 27 % of the total discharge and  $189 \text{ km}^3$   
797 representing hardly 12% of the total discharge to the Bay of Bengal (Table 8). Hence, our sampling coverage is  
798 higher in the Arabian Sea compared to Bay of Bengal during the wet period. Moreover, we did not sample  
799 Ganges-Brahmaputra, the largest river in the eastern coast draining into Bay of Bengal. In order to nullify the

800 sampling effects we propose to extrapolate the non-conservative behaviour of the flux to the total discharge into  
801 Bay of Bengal (1600 km<sup>3</sup>) and Arabian Sea (300 km<sup>3</sup>), taking into account the basin scale supply. Based on this  
802 extrapolation, we do indeed find a higher Si flux to the Bay of Bengal (211 ± 32, 10 ± 5, 2028 ± 317 Gmol) than  
803 to the Arabian Sea (80 ± 15, 7 ± 1, 1717 ± 932 Gmol) for DSi, ASi and LSi, respectively (Table 8). These Si  
804 fluxes calculated to the northern Indian Ocean (tropical side) might help to estimate the global coastal Si budget  
805 in the future.

806

## 807 **5. Conclusions**

808

809 1) Indian estuaries are highly diversified in terms of geographical situation (climate), topography, runoff and  
810 land-use practices. In this study, we have looked at the variability of amorphous, lithogenic and dissolved silicon  
811 as well as that of the main biogeochemical parameters relevant to Si, in several Indian estuaries in wet and dry  
812 seasons. Overall, we show that 40% of the ASi variability in dry season is explained by diatoms while lithogenic  
813 supply explains most of the ASi variability during high discharge. However, the strengths of the processes  
814 responsible for the variability of LSi and ASi are not clearly evidenced when looking at the dataset as a whole  
815 nor when applying a categorisation based only on location (NE, NW, SE, SW). Therefore, we separated our data  
816 into two categories i) upper (salinity <5), and ii) lower estuaries (salinity >5) for dry and wet period  
817 respectively. We then performed PCA and clustering on PCA results on these categories for each season. We  
818 show that during dry period in the upper estuaries, diatom production is common, with possible dissolution in the  
819 eastern and some western estuaries. In addition, a strong lithogenic impact was observed in the northeast  
820 (especially Haldia) and the northwest (e.g. Tapti) estuaries. For the remaining estuaries, there was no clear  
821 process explaining Si variability of the entire estuary. By nature, different principal processes are observed in  
822 the upper and lower estuaries, due to different levels of seawater intrusion and anthropogenic activity over the  
823 extent of the estuary.

824

825 2) In the wet season, a strong control of erosion is observed in all estuaries. The monsoon-driven discharge is  
826 likely the main control of particulate concentrations, especially in the lower estuaries.

827

828 3) Agricultural land use played a major role in the Si biogeochemical cycle, generally increasing fluxes in all  
829 forms - ASi, DSi and LSi. The southwestern estuaries, however, seem to expose a different behaviour, as Si  
830 fluxes appear related to the region's greater forest cover which prevents soil erosion. The present work is the  
831 first study on particle Si variability in estuaries at the Indian subcontinent scale and confirms that the silicon  
832 cycle is impacted by anthropogenic activities. Therefore, temporal monitoring of individual estuaries is  
833 necessary to better assess continuing changes to the Si cycle and its impact on the health of the estuarine and  
834 coastal ecosystems.

835

836 4) Our results show a strong seasonal effect on the variability of biogeochemical parameters along the salinity  
837 gradient and expose major differences among different estuaries. We extrapolate our data taking into account  
838 sampling coverage and non-conservativity within estuaries, to estimate DSi, ASi and LSi fluxes from Indian

839 subcontinent respectively as  $211 \pm 32$ ,  $10 \pm 5$ ,  $2028 \pm 317$  Gmol to the Bay of Bengal compared to  $80 \pm 15$ ,  $7 \pm$   
840  $1$  and  $1717 \pm 932$  Gmol to the Arabian Sea.

841

842 5) We show that the Si:N ratio was always above 1, (1 being the ratio needed for diatoms growth) across the  
843 entire salinity range and across seasonal and spatial differences. This could in part explain the absence of  
844 eutrophication prevailing in the Indian estuaries and their adjoining coastal seas.

845

#### 846 **Acknowledgements**

847

848 The research leading to these results has been mostly funded by the European Union Seventh Framework  
849 Program under grant agreement #294146 (MuSiCC Marie Curie CIG) and from the French National INSU  
850 programme EC2CO-LEFE (project SINDIA funded by Actions CYBER and BIOHEFFECT). K.R. Mangalaa  
851 scholarship has been mainly provided by the Erasmus Mundus Action 2 of the European Union (GATE project),  
852 with additional support from the Scientific Department of French Embassy in India and, MuSiCC. The authors  
853 would like to thank M. Benrahmoune (LOCEAN, CNRS) for managing the clean lab and performing  
854 colorimetric analyses. Special thanks to Bart Pattyn from Ranavision for extensive proofreading of the  
855 manuscript. We also thank the constructive and thorough comments from two anonymous reviewers, which  
856 helped in improving the paper.

857

#### 858 **6. References**

859

860 Admiraal, W., Breugem, P., Jacobs, D. M. L. H. a. & Steveninck, E. D. Fixation of dissolved silicate and  
861 sedimentation of biogenic silicate in the lower river Rhine during diatom blooms. *Biogeochemistry* **9**, 175–  
862 185 (1990).

863 Aigars, J., Jurgensone, I. & Jansons, M. Dynamics of silica and phytoplankton population under altered  
864 conditions of river flow in the Daugava River, Latvia. *Est. J. Ecol.* **63**, 217 (2014).

865 Anderson G. F. Silica, diatoms and a freshwater productivity maximum in Atlantic Coastal Plain estuaries,  
866 Chesapeake Bay. *Estuar. Coast. Shelf Sci.* **22**, 183–197, (1986).

867 Ansotegui, A. The Use of Pigment Signatures to Assess Phytoplankton Assemblage Structure in Estuarine  
868 Waters. *Estuar. Coast. Shelf Sci.* **52**, 689–703 (2001).

869 Attri, S. D. & Tyagi, A. Climate profile of India. *Gov. India Minist. Earth Sci.* **129** (2010). at  
870 [http://www.imd.gov.in/doc/climate\\_profile.pdf](http://www.imd.gov.in/doc/climate_profile.pdf).

871 Barão, L. Vandevenne, Floor. Clymans, Wim. Frings, Patrick. Ragueneau, Olivier. Meire, Patrick. Conley,  
872 Daniel J. Struyf, Eric. Alkaline-extractable silicon from land to ocean: A challenge for biogenic silicon  
873 determination. *Limnol. Oceanogr. Methods* **13**, 329–344 (2015).

874 Berner, R. A. Weathering, plants, and the long-term carbon cycle. *Geochimica et Cosmochimica Acta*, **56(8)**,  
875 3225–3231. (1992).

876 Bootsma, H. A., Hecky, R. E., Johnson, T. C., Kling, H. J. & Mwita, J. Inputs, Outputs, and Internal Cycling of  
877 Silica in a Large, Tropical Lake. *J. Great Lakes Res.* **29**, 121–138 (2003).

878 Brzezinski, M. A.: The si:c:N ratio of marine diatoms: Interspecific variability and the effect of some  
879 environmental variables, *J.phycol*, **21**, 347–357, 1985.

880 Carbonnel, V., Vanderborght, J. P., Lionard, M. & Chou, L. Diatoms, silicic acid and biogenic silica dynamics  
881 along the salinity gradient of the Scheldt estuary (Belgium/The Netherlands). *Biogeochemistry* **113**, 657–682  
882 (2013).

883 Cary, L., Alexandre, A., Meunier, J. D., Boeglin, J. L. & Braun, J. J. Contribution of phytoliths to the suspended  
884 load of biogenic silica in the Nyong basin rivers (Cameroon). *Biogeochemistry* **74**, 101–114 (2005).

885 Central water commission report. National Register of Large Dams – 2009. (2009).

886 Chou L. and R. Wollast. Estuarine silicon dynamics. In: *The Silicon Cycle. Human Perturbations and Impacts*  
887 *on Aquatic Systems*. Edited by V. Ittekkot, D. Unger, C. Humborg and N. Tac An. Scope **66**, pp. 93- 120,  
888 Island Press, Washington, Covelo, London (2006).

889 Clymans, W., Govers, G., Van Wesemael, B., Meire, P. & Struyf, E. Amorphous silica analysis in terrestrial  
890 runoff samples. *Geoderma* **167–168**, 228-235 (2011).

891 Commission, C. W., Remote, N. & Centre, S. Watershed Atlas. (2014).

892 Conley, D. J. An interlaboratory comparison for the measurement of biogenic silica in sediments. 39–48 (1998).

893 Conley, D. J. Likens, Gene E. Buso, Donald C. Saccone, Loredana. Bailey, Scott W. Johnson, Chris E.  
894 Deforestation causes increased dissolved silicate losses in the Hubbard Brook Experimental Forest. *Glob.*  
895 *Chang. Biol.* **14**, 2548–2554 (2008).

896 Conley, D. J. Riverine contribution of biogenic silica to the oceanic silica budget. *Limnol. Oceanogr.* **42**, 774–  
897 777 (1997).

898 Conley, D. J. Terrestrial ecosystems and the global biogeochemical silica cycle. *Global Biogeochem. Cycles* **16**,  
899 1–8 (2002).

900 Conley, D. J., Schelske, C. L. & Stoermer, E. F. Modification of the biogeochemical cycle of silica with  
901 eutrophication. *Mar. Ecol. Prog. Ser.* **101**, 179–192 (1993).

902 Delvaux, C. Cardinal, D. Carbonnel, V. Chou, L. Hughes, H.J. André, L. Controls on riverine  $\delta^{30}\text{Si}$  signatures  
903 in a temperate watershed under high anthropogenic pressure (Scheldt — Belgium). *J. Mar. Syst.* 1–12  
904 (2013).

905 Ducklow, H. W., Steinberg, D. K. & Buesseler, K. O. Upper ocean carbon export and the biological pump.  
906 *Oceanography* **14**, 50–58 (2001).

907 Dunne, T. Rates of chemical denudation of silicate rocks in tropical catchments. *Nature* **274**, 244–246 (1978).

908 Durga bharathi. Variability in composition and diversity of phytoplankton in the Indian estuaries and coastal  
909 Bay of Bengal. Ph.D. thesis (2014).

910 Dürr, H. H., Meybeck, M., Hartmann, J., Laruelle, G. G. & Roubeix, V. Global spatial distribution of natural  
911 riverine silica inputs to the coastal zone. *Biogeosciences* **8**, 597–620 (2011).

912 Friedl, G., Teodoru, C. & Wehrli, B. Is the Iron Gate I reservoir on the Danube River a sink for dissolved silica?  
913 *Biogeochemistry* **68**, 21–32 (2004).

914 Frings, P. J. Clymans, Wim. Fontorbe, Guillaume. Gray, William. Chakrapani, Govind J. Conley, Daniel J. De  
915 La Rocha, Christina. Silicate weathering in the Ganges alluvial plain. *Earth Planet. Sci. Lett.* **427**, 136–148  
916 (2015).

917 Frings, P. J., Clymans, W. & Conley, D. J. Amorphous Silica Transport in the Ganges Basin: Implications for Si  
918 Delivery to the Oceans. *Procedia Earth Planet. Sci.* **10**, 271–274 (2014).

919 Garnier, J., Beusen, A., Thieu, V., Billen, G. & Bouwman, L. N:P:Si nutrient export ratios and ecological  
920 consequences in coastal seas evaluated by the ICEP approach. *Global Biogeochem. Cycles* **24**, GBOA05, 1–  
921 12 (2010).

922 Government of India. State of Indian Agriculture. 247 (2012). <http://agricoop.nic.in/sia111213312.pdf>.

923 Grasshoff K., K. Kremling, M. Ehrhardt. *Methods of Seawater Analysis 3<sup>rd</sup> Edition completely Revised. and*  
924 *Extended edition.* Wiley- VCH. ISBN 3-527-29589-5, (1999).

925 Gupta V.M. Garuda and Vongala V.Sarma: Biogenic silica in the Bay of Bengal, *Oceanol. acta*, **20**(3), 493–500,  
926 1997.

927 Gurumurthy, G. P. Balakrishna, K. Riotte, Jean Braun, Jean-Jacques Audry, Stéphane Shankar, H.N. Udaya  
928 Manjunatha, B.R. Controls on intense silicate weathering in a tropical river, southwestern India. *Chem. Geol.*  
929 **300-301**, 61–69 (2012).

930 Heiskanen, A. S. & Keck, A. Distribution and sinking rates of phytoplankton, detritus, and particulate biogenic  
931 silica in the Laptev Sea and Lena River (Arctic Siberia). *Mar. Chem.* **53**, 229–245 (1996).

932 Heukelem. Van, L. & Thomas, C. Computer-assisted high-performance liquid chromatography method  
933 development with applications to the isolation and analysis of phytoplankton pigments. *J. Chromatogr. A*  
934 **910**, 31–49 (2001).

935 Howarth, Robert Chan, Francis Conley, Daniel J Garnier, Josette Doney, Scott C Marino, Roxanne Billen,  
936 Gilles. Coupled biogeochemical cycles: eutrophication and hypoxia in temperate estuaries and coastal  
937 marine ecosystems. *Front. Ecol. Environ.* **9**, 18–26 (2011).

938 Hughes, H. J, Sondag Francis, Cocquyt Christine, Laraque Alain, Pandi Albert, André Luc, Cardinal Damien.  
939 Effect of seasonal biogenic silica variations on dissolved silicon fluxes and isotopic signatures in the Congo  
940 River. *Limnol. Oceanogr.* **56**, 551–561 (2011).

941 Hughes, H. J., Bouillon, S., André, L. & Cardinal, D. The effects of weathering variability and anthropogenic  
942 pressures upon silicon cycling in an intertropical watershed (Tana River, Kenya). *Chem. Geol.* **308-309**, 18–  
943 25 (2012).

944 Hughes, H. J., Sondag, F., Santos, R. V., André, L. & Cardinal, D. The riverine silicon isotope composition of  
945 the Amazon Basin. *Geochim. Cosmochim. Acta* **121**, 637–651 (2013).

946 Humborg, C, M. Pastuszak, Juris Aigars, H. Siegmund, C.-M. Morth and V. Ittekkot. Decreased Silica Land–sea  
947 Fluxes through Damming in the Baltic Sea Catchment – Significance of Particle Trapping and Hydrological  
948 Alterations. *Biogeochemistry* **77**, 265–281 (2006).

949 Ittekkot, V., R. R. Nair, S. Honjo, V. Ramaswamy, M. Bartsch, S. Manganini, and B. N. Desai. Enhanced  
950 particle fluxes in Bay of Bengal induced by injection of fresh water, *Nature*, **351**, 385–387. (1991).

951 Krishna, M. S. Prasad, M. H K. Rao, D. B. Viswanadham, R. Sarma, V. V S S. Reddy, N. P C. Export of  
952 dissolved inorganic nutrients to the northern Indian Ocean from the Indian monsoonal rivers during  
953 discharge period. *Geochim. Cosmochim. Acta* **172**, 430–443 (2016).

954 Laruelle, G. G. Roubex, V. Sferratore, A. Brodherr, B. Ciuffa, D. Conley, D. J. Dürr, H. H. Garnier, J.  
955 Lancelot, C. Le Thi Phuong, Q. Meunier, J.-D. Meybeck, M. Michalopoulos, P. Moriceau, B. Ni Longphuirt,  
956 S.Loucaides, S. Papush, L. Presti, M. Ragueneau, O. Regnier, P. Saccone, L. Slomp, C. P. Spiteri, C. Van



957 Cappellen, P. Anthropogenic perturbations of the silicon cycle at the global scale: Key role of the land-ocean  
958 transition. *Global Biogeochem. Cycles* **23**, 1–17 (2009).

959 Lehtimäki, M., Tallberg, P. & Siipola, V. Seasonal Dynamics of Amorphous Silica in Vantaa River Estuary.  
960 *Silicon* **5**, 35–51 (2013).

961 Li, M., Xu, K., Watanabe, M. & Chen, Z. Long-term variations in dissolved silicate, nitrogen, and phosphorus  
962 flux from the Yangtze River into the East China Sea and impacts on estuarine ecosystem. *Estuar. Coast.*  
963 *Shelf Sci.* **71**, 3–12 (2007).

964 Liu, S. M., Hong, G.-H., Ye, X. W., Zhang, J. & Jiang, X. L. Nutrient budgets for large Chinese estuaries and  
965 embayment. *Biogeosciences Discuss.* **6**, 391–435 (2009).

966 Lu, C. A. O., Sumei, L. I. U. & Jingling, R. E. N. Seasonal variations of particulate silicon in the Changjiang  
967 (Yangtze River) Estuary and its adjacent area. *Acta Oceanol. Sin.* **32**, 1–10 (2013).

968 Meunier, J. D. Riotte, J. Braun, J.J. Sekhar, M. Chalié, F. Barboni, D. Saccone, L. Controls of DSi in streams  
969 and reservoirs along the Kaveri River, South India. *Sci. Total Environ.* **502**, 103–113 (2015).

970 Middelburg, J. J. & Herman, P. M. J. Organic matter processing in tidal estuaries. *Mar. Chem.* **106**, 127–147  
971 (2007).

972 Nair, R. R, V. Ittekkot, S. J. Managanini , V. Ramaswamy, B. Hakke, E.T. Degens, B. N. Desai and S. Honjo,  
973 Increased particle flux to the deep ocean related to monsoon, *Nature*, **338**, 749–751, (1989).

974 Nayak, G. N. & Hanamgond, P. T. India. *Encycl. World's Coast. Landforms* **2010**, 1065–1070 (2010).

975 Naqvi, S. W. A., Moffett, J. W., Gauns, M. U., Narvekar, P. V., Pratihary, A. K., Naik, H., Shenoy, D. M.,  
976 Jayakumar, D. A., Goepfert, T. J., Patra, P. K., Al-Azri, A. and Ahmed, S. I.: The Arabian Sea as a high-  
977 nutrient, low-chlorophyll region during the late Southwest Monsoon, *Biogeosciences*, 7(7), 2091–2100,  
978 doi:10.5194/bg-7-2091-2010, 2010.

979 Nelson, D. M., Tréguer, P., Brzezinski, M. A., Leynaert, A. & Quéguiner, B. Production and dissolution of  
980 biogenic silica in the ocean: Revised global estimates, comparison with regional data and relationship to  
981 biogenic sedimentation. *Global Biogeochem. Cycles* **9**, 359–372 (1995).

982 Ragueneau, Olivier. Savoye, Nicolas. Del Amo, Yolanda. Cotten, Jo. Tardiveau, Benoît. Leynaert, Aude. Del,  
983 Yolanda. Cotten, Jo. A new method for the measurement of biogenic silica in suspended matter of coastal  
984 waters: using Si:Al ratios to correct for the mineral interference. *Cont. Shelf Res.* **25**, 697–710 (2005).

985 Ragueneau, O. Treguer P, Leynaert A, Anderson R F, Brzezinski MA, De Master D J. A review of the Si cycle  
986 in the modern ocean: Recent progress and missing gaps in the application of biogenic opal as a  
987 paleoproductivity proxy. *Glob. Planet. Change* **26**, 317–365 (2000).

988 Raimonet M., Andrieux-Loyer F., Ragueneau O., Michaud E., Kerouel R., Philippon X., Nonent M., Mémery,  
989 L. Strong gradient of benthic biogeochemical processes along a macrotidal temperate estuary: focus on P and  
990 Si cycles. *Biogeochemistry* (2013).

991 Ran, XiangBin. Che, Hong. Zang, JiaYe. Yu, Yong Gui. Liu, Sen. Zheng, LiLi. Variability in the composition  
992 and export of silica in the Huanghe River Basin. *Sci. China Earth Sci.* (2015).

993 Rao, G. D. and Sarma V. V. S. S. Contribution of N<sub>2</sub>O emissions to the atmosphere from Indian monsoonal  
994 estuaries. *Tellus, Ser. B Chem. Phys. Meteorol.* **1**, 1–9 (2013).

995 Sarma, V. V. S. S. Viswanadham, R. Rao, G. D. Prasad, V. R. Kumar, B. S. K. Naidu, S. a. Kumar, N. a. Rao, D.  
996 B. Sridevi, T. Krishna, M. S. Reddy, N. P. C. Sadhuram, Y. Murty, T. V. R. Carbon dioxide emissions from  
997 Indian monsoonal estuaries. *Geophys. Res. Lett.* **39**, (2012).

998 Sarma, V. V. S. S. M.S. Krishna, V.R. Prasad, B.S.K. Kumar, S.A. Naidu, G.D. Rao, R. Viswanadham, T.  
999 Sridevi, P.P. Kumar, N.P.C. Reddy. Distribution and sources of particulate organic matter in the Indian  
1000 monsoonal estuaries during monsoon. **119**, 1–17 (2014).

1001 Sarma, V. V. S. S. S.N.M. Gupta, P.V.R. Babu, T. Acharya, N. Harikrishnachari, K. Vishnuvardhan, N.S. Rao,  
1002 N.P.C. Reddy, V.V. Sarma, Y. Sadhuram, T.V.R. Murty, M.D. Kumar. Influence of river discharge on  
1003 plankton metabolic rates in the tropical monsoon driven Godavari estuary, India. *Estuar. Coast. Shelf Sci.*  
1004 **85**, 515–524 (2009).

1005 Sarma, V. V. S. S., Sridevi, B., Maneesha, K., Sridevi, T., Naidu, S. A., Prasad, V. R., Venkataramana, V.,  
1006 Acharya, T., Bharati, M. D., Subbaiah, C. V., Kiran, B. S., Reddy, N. P. C., Sarma, V. V., Sadhuram, Y. and  
1007 Murty, T. V. R.: Impact of atmospheric and physical forcings on biogeochemical cycling of dissolved  
1008 oxygen and nutrients in the coastal Bay of Bengal, *J. Oceanogr.*, **69**(2), 229–243, doi:10.1007/s10872-012-  
1009 0168-y, (2013).

1010 Schoelhamer, D.H., Influence of salinity, bottom topography, and tides on locations of estuarine turbidity  
1011 maxima in northern San Francisco Bay, in McAnally, W.H. and Mehta, A.J., ed., *Coastal and Estuarine Fine  
1012 Sediment Transport Processes*: Elsevier Science B.V., p. 343-357, (2001).

1013 Sharma. S.K and V. Subramanian. Hydrochemistry of the Narmada and Tapti Rivers, India. *Hydrol. Process.*  
1014 **22**, 3444–3455 (2008).

1015 Shynu, R., Purnachandra Rao, V., Sarma, V. V. S. S., Kessarkar, P. M. and Mani Murali, R.: Sources and fate of  
1016 organic matter in suspended and bottom sediments of the Mandovi and Zuari estuaries, western India, *Curr.*  
1017 *Sci.*, **108**(2), 226–238, 2015.

1018 Soman, M. K. & Kumar, K. K. Some aspects of daily rainfall distribution over India during the south-west  
1019 monsoon season. *Int. J. Climatol.* **10**, 299–311 (1990).

1020 Sridevi, B., Sarma, V. V S S., Murty, T. V R., Sadhuram, Y., Reddy, N. P C., Vijayakumar, K., Raju, N. S.N.,  
1021 Jawahar Kumar, C. H., Raju, Y. S N., Luis, R., Kumar, M. D., Prasad, K. V S R. Variability in stratification  
1022 and flushing times of the Gautami–Godavari estuary, India. *J. Earth Syst. Sci.* **124**, 993–1003 (2015).

1023 Struyf, E., Van Damme, S., Gribsholt, B., Middelburg, J. J. & Meire, P. Biogenic silica in tidal freshwater marsh  
1024 sediments and vegetation (Schelde estuary, Belgium). *Mar. Ecol. Prog. Ser.* **303**, 51–60 (2005).

1025 Struyf, E., Dausse, A., Van Damme, S., Bal, K., Gribsholt, B., Boschker, H. T. S., Middelburg, J. J. and Meire,  
1026 P.: Tidal marshes and biogenic silica recycling at the land-sea interface, *Limnol. Oceanogr.*, **51**(2), 838–846,  
1027 doi:10.4319/lo.2006.51.2.0838, 2006.

1028 Struyf, E. Adriaan Smis, Stefan Van Damme, Josette Garnier, Gerard Govers, Bas Van Wesemael, Daniel J.  
1029 Conley, Okke Batelaan, Elisabeth Frot, Wim Clymans, Floor Vandevenne, Christiane Lancelot, Peter Goos  
1030 & Patrick Meire. Continental Historical land use change has lowered terrestrial silica mobilization. *Nat.*  
1031 *Commun.* 1:129 doi: 10.1038/ncomms1128 (2010).

1032 Subramanian V., V. Ittekkot, D. Unger, N. Madhavan. Silicate weathering in South Asian tropical river basins.  
1033 In: *The Silicon Cycle, Human perturbations and impacts on aquatic system* (Eds.: V. Ittekkot, D. Uner, C.H.  
1034 Humborg, N. Tac An). SCOPE Report 66, Island Press, 3-12, (2006).

1035 Suja, S., Kessarkar, P. M., Shynu, R., Rao, V. P. and Fernandes, L. L.: Spatial distribution of suspended  
1036 particulate matter in the Mandovi and Zuari estuaries: Inferences on the estuarine turbidity maximum, *Curr.*  
1037 *Sci.*, **110**(7), 1165–1168, 2016.

1038 Sun, X., Andersson, P. S., Humborg, C., Pastuszak, M. & Mörth, C. M. Silicon isotope enrichment in diatoms  
1039 during nutrient-limited blooms in a eutrophied river system. *J. Geochemical Explor.* **132**, 173–180 (2013).

1040 Tréguer, P. Nelson, D M, Van Bennekom, a J, Demaster, D J, Leynaert, A, Quéguiner, B . The silica balance in  
1041 the world ocean: a re-estimate. *Science* **268**, 375–379 (1995).

1042 Tréguer, P. J. & De La Rocha, C. L. The world ocean silica cycle. *Ann. Rev. Mar. Sci.* **5**, 477–501 (2013).

1043 Vijith, V., Sundar, D. & Shetye, S. R. Time-dependence of salinity in monsoonal estuaries. *Estuar. Coast. Shelf*  
1044 *Sci.* **85**, 601–608 (2009).

1045 Wedepohl, K. H. INGERSON LECTURE The composition of the continental crust. *Geochim. Cosmochim. Acta*  
1046 **59**, 1217–1232 (1995).

1047 Wu, J. T. & Chou, T. L. Silicate as the limiting nutrient for phytoplankton in a subtropical eutrophic estuary of  
1048 Taiwan. *Estuar. Coast. Shelf Sci.* **58**, 155–162 (2003).

1049 Wysocki, L. A., Bianchi, T. S., Powell, R. T. & Reuss, N. Spatial variability in the coupling of organic carbon,  
1050 nutrients, and phytoplankton pigments in surface waters and sediments of the Mississippi River plume.  
1051 *Estuar. Coast. Shelf Sci.* **69**, 47–63 (2006).

1052 Xue Jianhong, Cindy Lee, Stuart G.Wakeham, Robert. A. Armstrong.: Using principal components analysis  
1053 (PCA) with cluster analysis to study the organic geochemistry of sinking particles in the ocean, *Org.*  
1054 *Geochem.*, 42, 356–367 (2011).

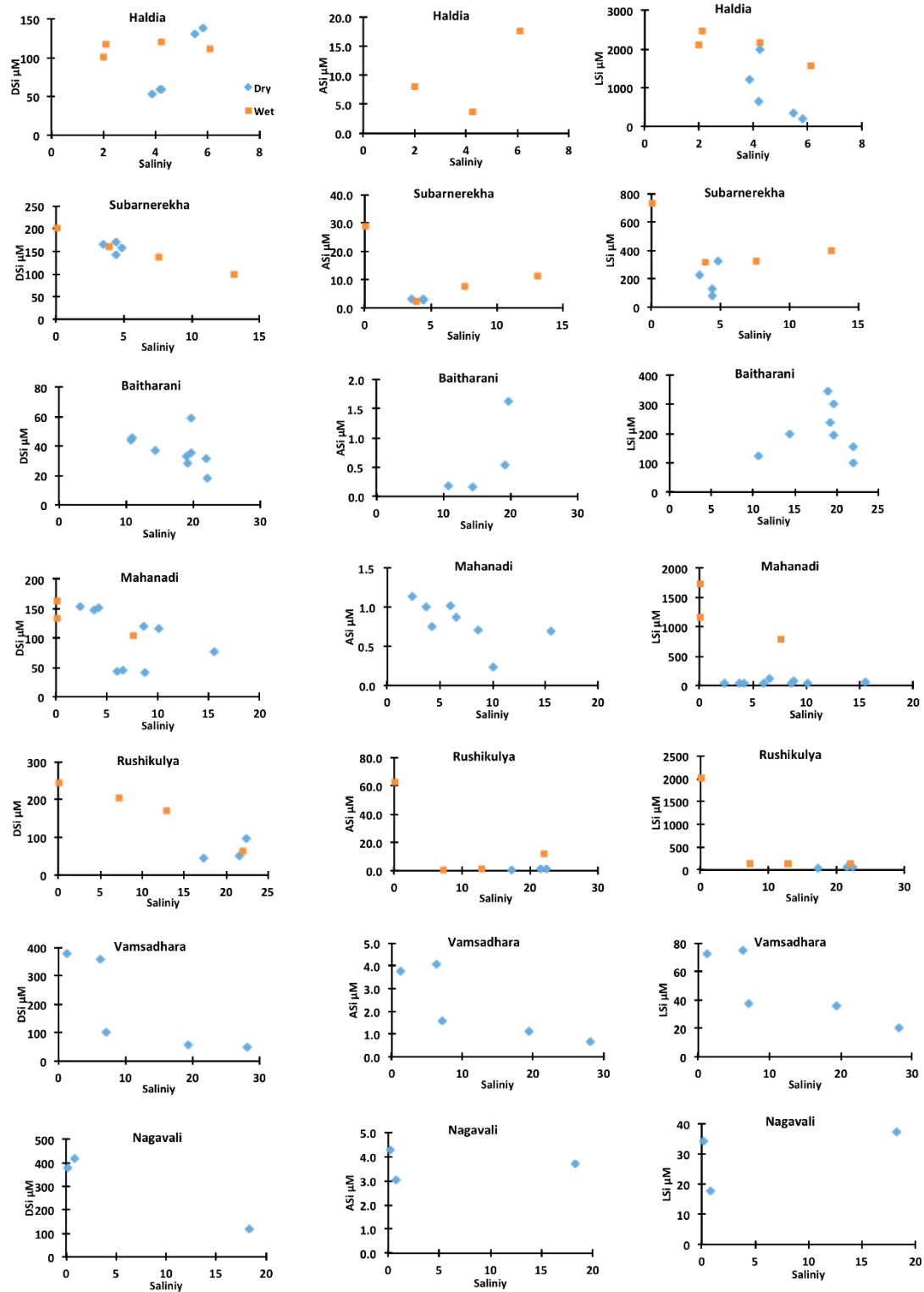
1055 Zhang. A.Y, J. Zhang, J.Hu, R. F. Zhang, and G. S. Z. School. *Journal of Geophysical Research: Oceans. J.*  
1056 *Geophys. Res. Ocean. Res.* 1–16 (2015).

1057 Zhu, Z.-Y. Ng, Wai-Man. Liu, Su-Mei. Zhang, Jing. Chen, Jay-Chung. Wu, Ying. Estuarine phytoplankton  
1058 dynamics and shift of limiting factors: A study in the Changjiang (Yangtze River) Estuary and adjacent area.  
1059 *Estuar. Coast. Shelf Sci.* **84**, 393–401 (2009).

1060

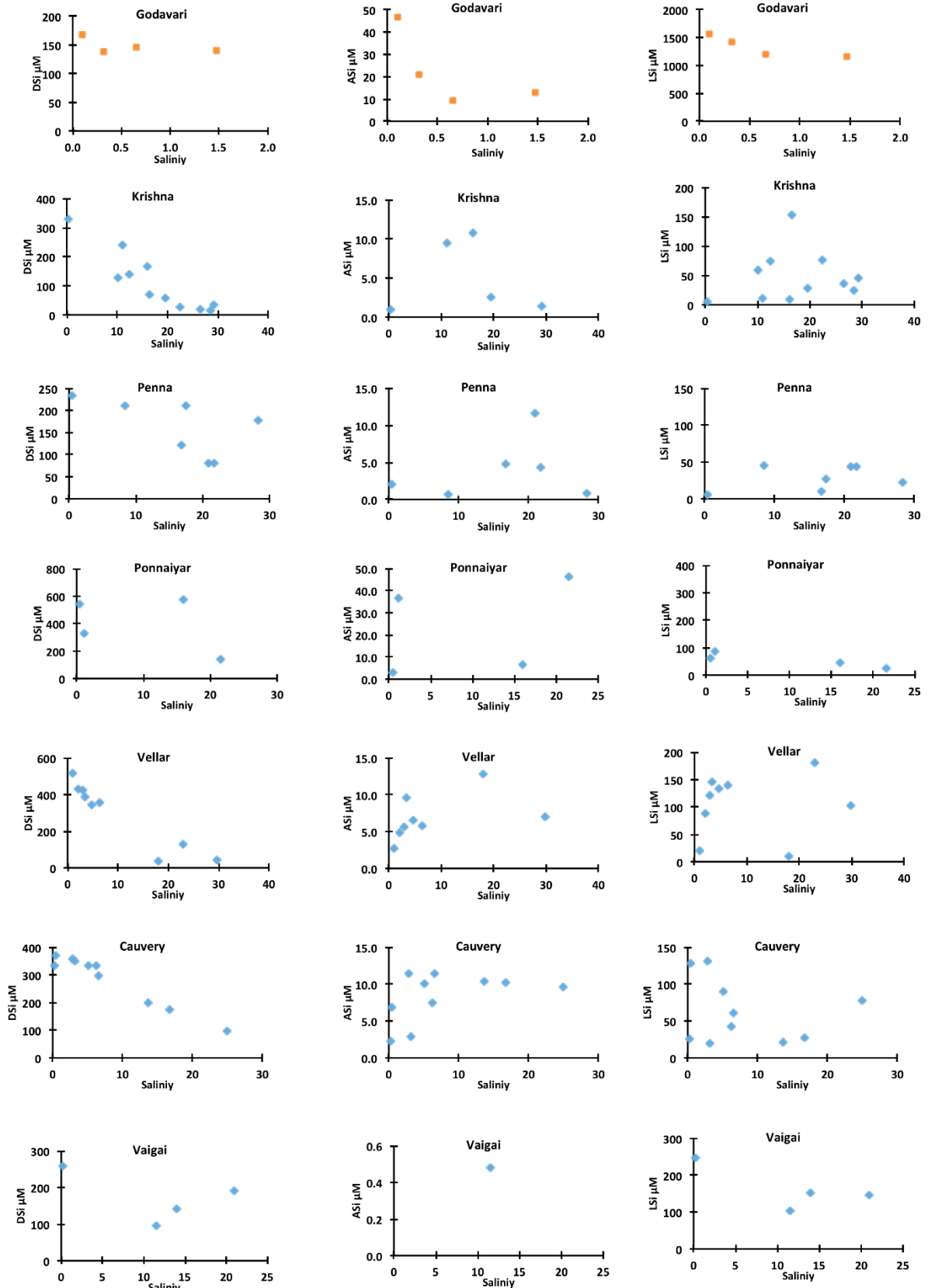
1061  
 1062  
 1063  
 1064

APPENDIXES  
 Appendix A  
 Individual samples data



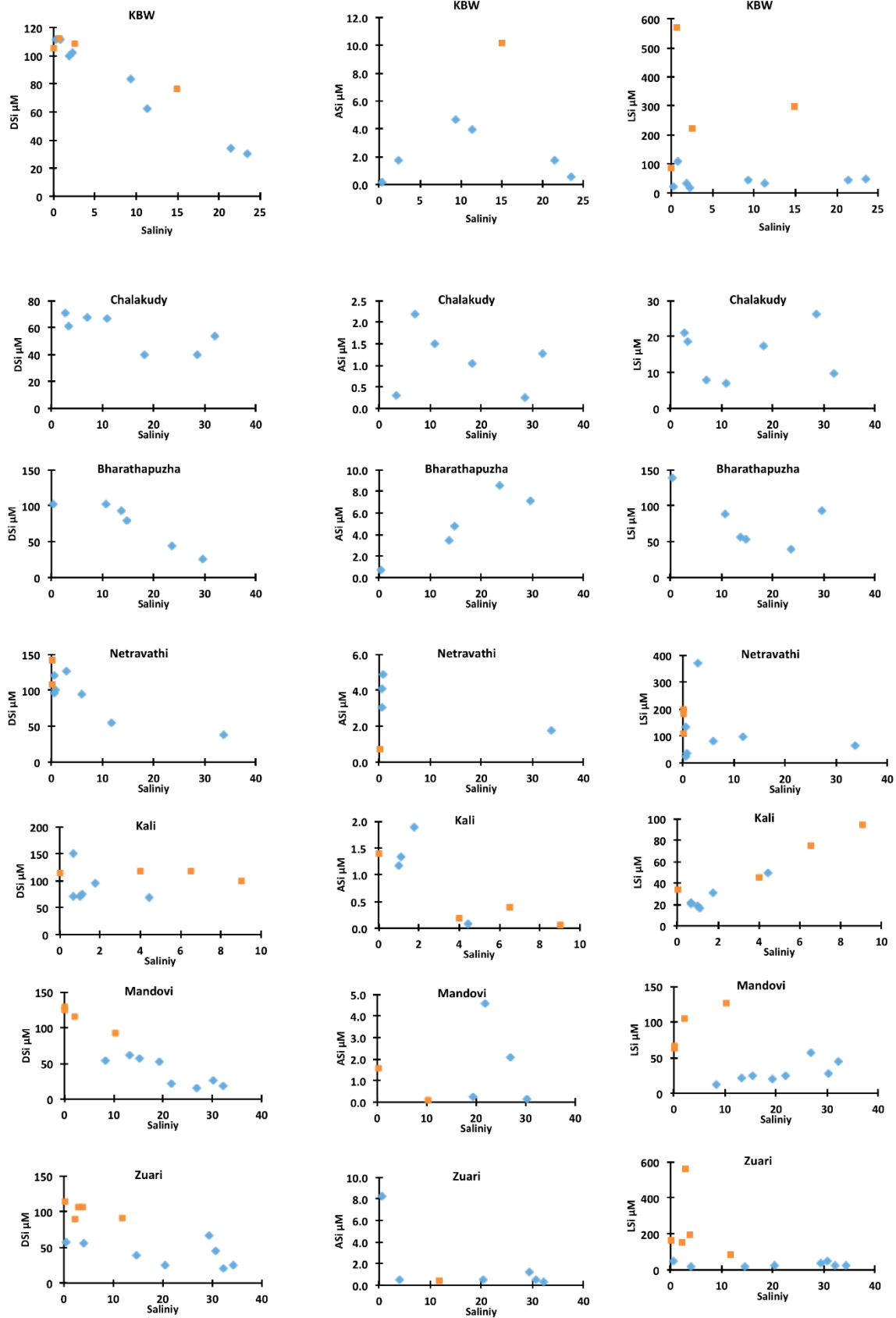
1065  
 1066  
 1067

**Fig. A1** DSi, ASi and LSi vs. salinity for northeast estuaries (wet season: orange squares, dry season: blue diamonds).



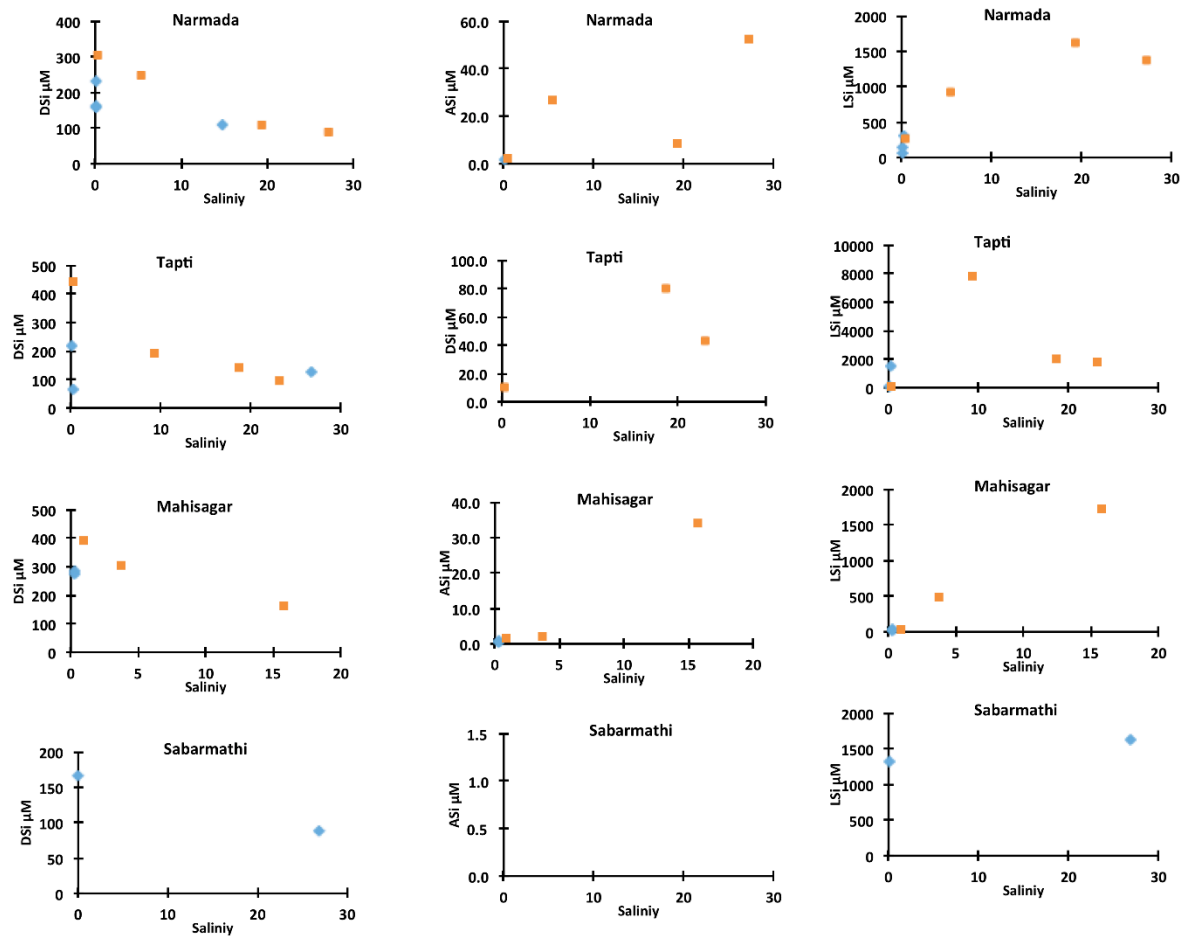
1068

1069 **Fig. A2** *DSi, ASi and LSi vs. salinity for southeast estuaries (wet season: orange squares, dry season: blue*  
 1070 *diamonds).*



1071

1072 **Fig. A3** *DSi, Asi and LSi vs. salinity for southwest estuaries (wet season: orange squares, dry season: blue*  
 1073 *diamonds).*



1074

1075 **Fig. A4** DSi, ASi and LSi vs. salinity for northwest estuaries (wet season: orange squares, dry season: blue  
 1076 diamonds).

1077

1078

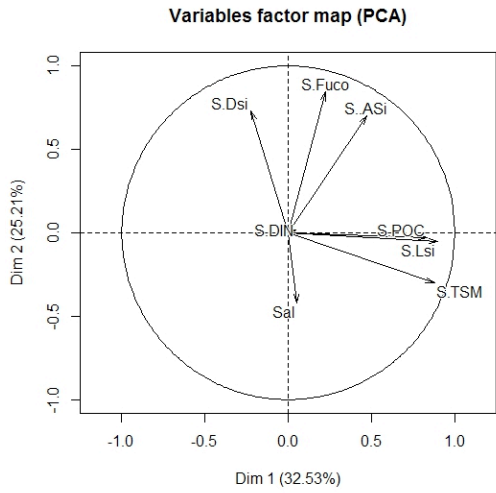
1079

1080

1081 **DRY period**

**Appendix B**

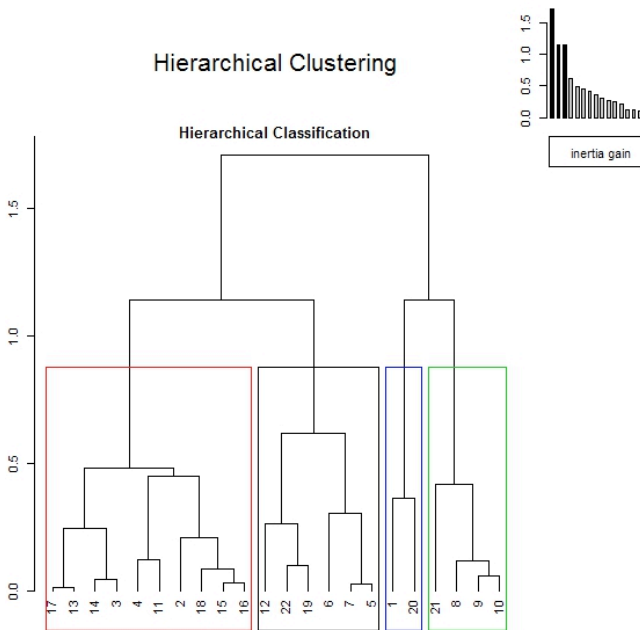
**Additional PCA and clustering figures and tables**



1082

1083 **Fig. B1:** PCA analysis on upper estuaries during dry period.

1084



1085

1086

1087 **Fig. B2** Hierarchical clustering of PCA results on upper estuaries during dry period.

1088

1089

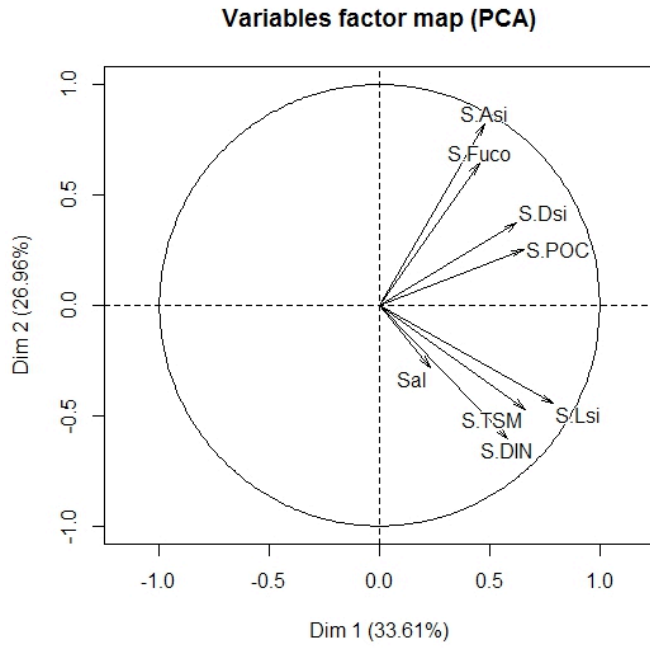
1090

1091

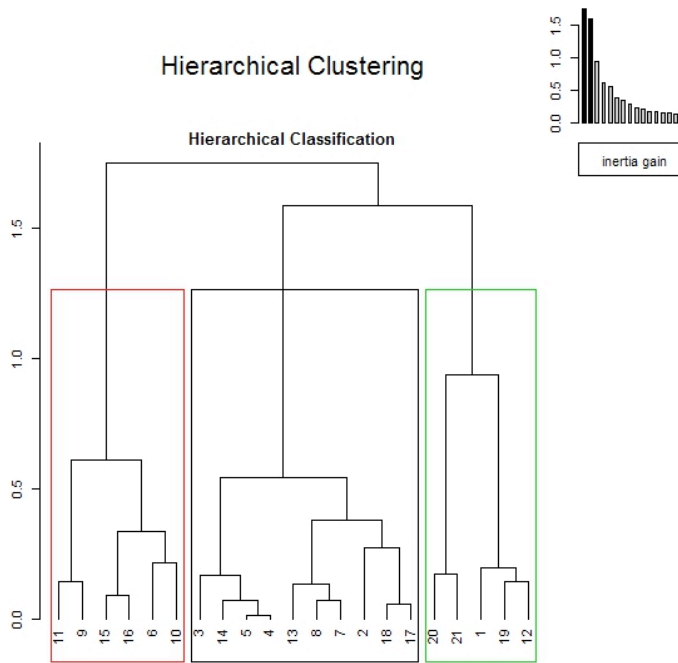
1092

1093



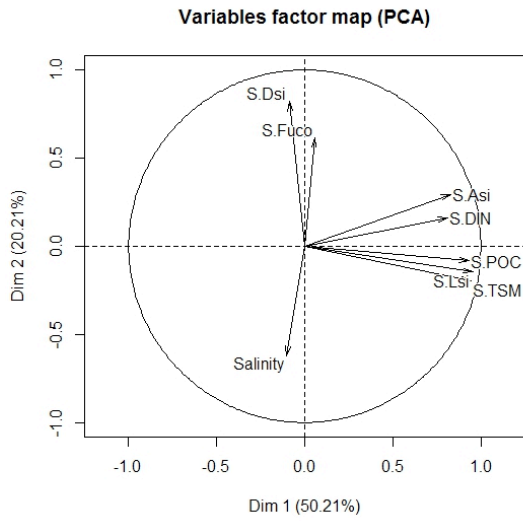


1094  
 1095 **Fig. B3:** PCA analysis on lower estuaries during dry period.  
 1096



1097  
 1098 **Fig. B4:** Hierarchical clustering of PCA results on lower estuaries during dry period.  
 1099

1100  
 1101  
 1102  
 1103 **Wet period**

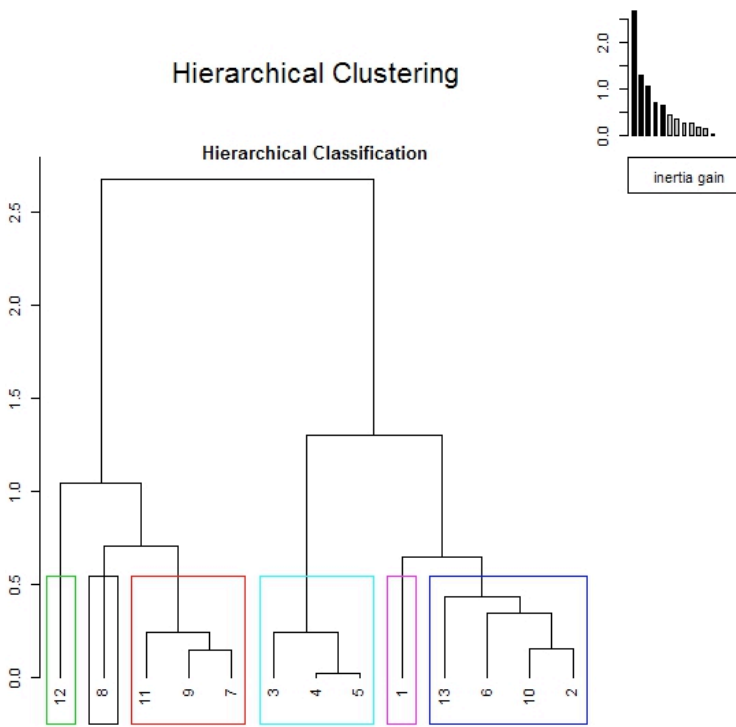


1104

1105 **Fig B5:** PCA analysis on upper estuaries during wet period.

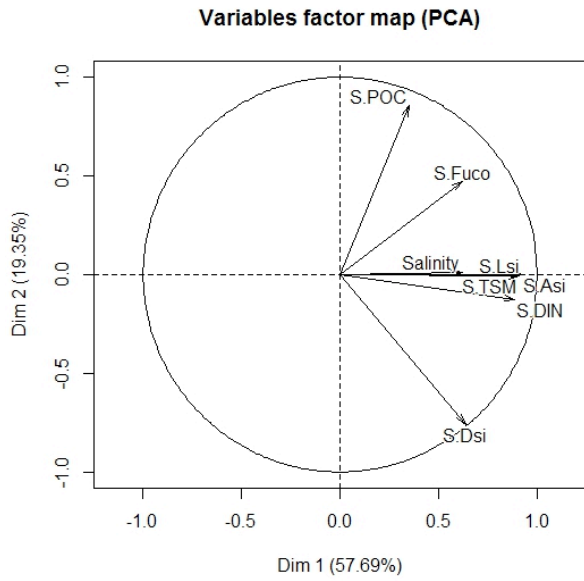
1106

1107



1108

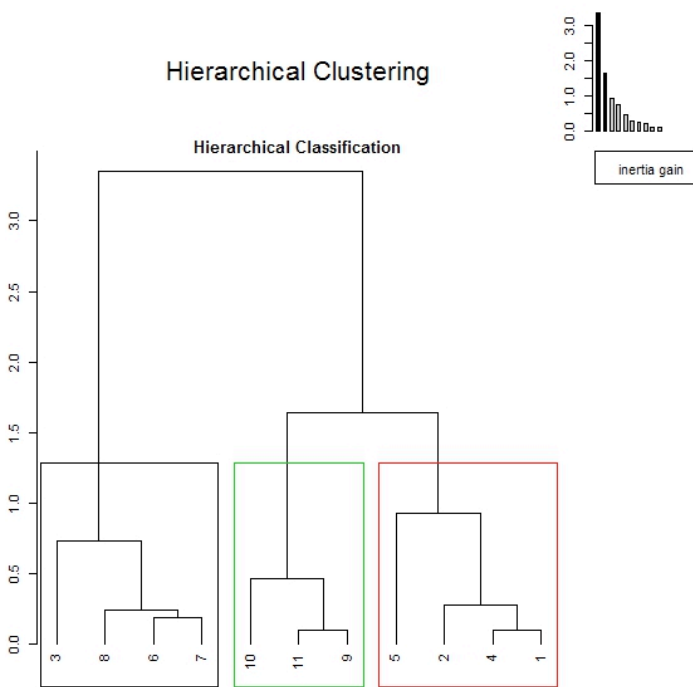
1109 **Fig. B5:** Hierarchical clustering of PCA results on upper estuaries during wet period.



1110

1111 **Fig. B6:** PCA analysis on lower estuaries during wet period

1112



1113

1114 **Fig.B7:** Hierarchical clustering of PCA results on lower estuaries during wet period.

1115

1116

1117

1118

1119

1120

1121 **Data used for PCA and clustering**

Ind.no	Estuary	Sal	DSi ( $\mu\text{M}$ )	TSM (mg/l)	POC ( $\mu\text{M}$ )	DIN ( $\mu\text{M}$ )	ASi ( $\mu\text{M}$ )	LSi ( $\mu\text{M}$ )	Fuco ( $\mu\text{g/l}$ )
1	Haldia-Hal	4.1	57	206	258	28	1.9	1280	0.3
2	Subernareka- Sub	4.3	159	30	103	9	7.0	189	1.5
3	Mahanadi-Maha	3.4	151	21	75	6	1.0	38	0.2
4	Vamsadhara-Vam	1.8	368	13	65	3	3.9	74	0.4
5	Nagavalli-Nag	0.5	399	9	47	13	3.7	26	2.2
6	Krishna-kri	0.4	327	3	61	75	0.9	6	NA
7	Penna-Pen	0.6	218	7	45	13	2.6	26	2.5
8	Ponnaiyar-Pon	1.1	494	84	167	7	13.3	63	6.7
9	Cauvery-Cau	2.3	348	21	98	8	6.7	79	5.3
10	Vellar-vel	2.8	423	46	172	17	5.9	102	2.9
11	Ambullar-Amb	4.2	317	17	95	7	2.5	40	0.2
12	Vaigai-Vai	0.2	258	85	124	10	1.8	246	0.1
13	KBW	1.3	106	66	51	18	1.6	45	0.8
14	Chalakudy-Cha	3.0	66	31	56	6	1.1	20	0.2
15	Bharathapuzha-Bha	1.8	99	45	84	8	2.1	95	1.3
16	Netravathi-Net	1.2	110	30	74	5	3.9	141	1.6
17	Kali	1.6	89	63	55	20	1.4	26	0.4
18	Zuari-Zua	2.3	57	63	65	11	4.4	34	2.0
19	Narmada-Nar	0.1	183	22	NA	34	2.3	171	0.7
20	Tapti-Tap	0.2	142	288	916	23	2.7	772	1.3
21	Sabarmati-Sab	0.0	166	84	NA	39	6.5	1330	5.2
22	Mahisagar-Mahi	0.2	278	28	NA	82	0.7	42	0.8

1122

1123 *Table B1: upper estuaries- dry period.*

1124

Ind.no	Estuary	Sal	DSi ( $\mu\text{M}$ )	TSM (mg/l)	POC ( $\mu\text{M}$ )	DIN ( $\mu\text{M}$ )	ASi ( $\mu\text{M}$ )	LSi ( $\mu\text{M}$ )	Fuco ( $\mu\text{g/l}$ )
1	Haldia-Hal	5.7	134	48	192	30	2.1	268	0.4
2	Baitharani-Bai	17.5	37	56	135	10	1.4	207	0.7
3	Mahanadi-Maha	9.3	74	14	52	6	0.9	61	0.4
4	Rushikulya-Rus	20.4	63	27	57	7	1.4	54	0.4
5	Vamsadhara-Vam	18.2	69	27	56	5	1.1	31	0.6
6	Nagavalli-Nag	18.3	118	7	97	10	3.7	37	1.7
7	Krishna-kri	17.4	102	58	52	17	4.0	57	1.3
8	Penna-Pen	16.7	101	19	32	14	4.4	41	1.6
9	Ponnaiyar-Pon	21.5	178	56	223	13	25.6	187	12.3
10	Cauvery-Cau	12.5	233	25	89	5	10.5	44	5.1
11	Vellar-vel	19.3	143	62	169	8	7.2	108	2.7
12	Vaigai-Vai	15.4	142	60	124	10	1.4	134	0.5
13	KBW	15.5	53	86	51	8	2.7	42	2.8
14	Chalakudy-Cha	19.3	53	11	49	7	1.2	14	0.6
15	Bharathapuzha-Bha	19.8	49	19	111	2	6.8	62	0.9
16	Netravathi-Net	17.1	63	27	75	3	5.0	81	4.1
17	Zuari-Zua	26.9	37	46	67	10	1.5	29	1.4
18	Mandovi-Man	20.9	38	42	45	12	2.0	29	2.4
19	Narmada-Nar	14.7	108	NA	NA	46	1.2	NA	NA
20	Tapti-Tap	26.7	125	49	NA	42	2.5	2635	0.9
21	Sabarmati-Sab	26.9	89	334	NA	60	1.4	1633	NA

1125

1126 *Table B2: Lower estuaries- dry period.*

1127

Ind.no	Estuary	Sal	DSi ( $\mu\text{M}$ )	TSM (mg/l)	POC ( $\mu\text{M}$ )	DIN ( $\mu\text{M}$ )	ASi ( $\mu\text{M}$ )	LSi ( $\mu\text{M}$ )	Fuco ( $\mu\text{g/l}$ )
1	Haldia-Hal	2.8	113	617	131	34	5.9	2241	0.4
2	Subernarekha-Sub	2.0	181	74	51	11	15.7	526	0.4
3	Rushikulya-Rus	0.1	242	278	91	35	62.8	2001	0.1
4	Mahanadi-Maha	0.1	149	209	68	40	32.6	1442	NA
5	Godavari-God	0.6	147	200	76	54	22.3	1338	NA
6	KBW	1.1	109	46	105	45	5.5	293	0.4
7	Netravathi-Net	0.1	130	30	29	24	2.6	164	0.5
8	Kali	2.0	116	9	17	5	0.8	39	0.1
9	Mandovi-Man	0.7	123	17	21	18	1.2	78	0.2
10	Zuari-Zua	2.3	104	46	38	21	5.4	270	0.5
11	Narmada-Nar	0.4	305	42	27	13	2.5	266	0.3
12	Tapti-Tap	0.3	443	13	36	18	9.8	57	1.7
13	Mahisagar-Mahi	2.3	347	42	34	32	1.8	262	0.5

1128

1129 *Table B3: Upper estuaries- wet period.*

1130

1131

Ind.no	Estuary	Sal	DSi ( $\mu\text{M}$ )	TSM (mg/l)	POC ( $\mu\text{M}$ )	DIN ( $\mu\text{M}$ )	ASi ( $\mu\text{M}$ )	LSi ( $\mu\text{M}$ )	Fuco ( $\mu\text{g/l}$ )
1	Haldia-Hal	6.1	112	414	NA	14	17.6	1582	0.5
2	Subernarekha-Sub	10.3	119	60	31	26	9.5	360	0.9
3	Rushikulya-Rus	14.0	146	28	16	14	4.6	138	0.5
4	Mahanadi-Maha	7.6	105	137	NA	5	9.9	796	NA
5	KBW	14.9	77	62	84	16	10.1	297	1.4
6	Kali	7.8	109	21	25	7	0.2	85	0.2
7	Mandovi-Man	10.3	92	29	34	7	0.1	127	NA
8	Zuari-Zua	11.8	91	22	31	1	0.4	85	0.3
9	Narmada-Nar	19.4	149	431	51	44	29.4	1299	0.5
10	Tapti-Tap	17.0	145	596	NA	53	61.4	3881	2.3
11	Mahisagar-Mahi	15.8	162	368	NA	53	34.0	1737	0.4

1132

1133 *Table B4: lower estuaries- wet period.*

1134

1135

1136

1137

1138